ADDIS ABABA UNIVERSITY

ADDIS ABABA INSTITUTE OF TECHNOLOGY

SCHOOL OF MECHANICAL AND INDUSTRIAL ENGINEERING

GRADUATE PROGRAM IN RAILWAY ENGINEERING

FATIGUE ANALYSIS OF AALRT BOLTED RAIL JOINT

A RESEARCH PAPER SUBMITTED TO THE ADDIS ABABA INSTITUTE OF

TECHNOLOGY, SCHOOL OF GRADUATE STUDIES, ADDIS ABABA UNIVERSITY FOR PARTIAL FULFILLMENT OF THE REQUIREMENTS FOR MASTER OF SCIENCE IN ROLLING STOCK ENGINEERING.

BY

JEMIL DEGIFE

ADVISOR:

ATO TOLLOSSA DEBERIE

March, 2015

Approved By Board of Examiners

1.	Ato Tollossa Deberie	_____	_____
	Advisor	Signature	Date
2.	Ato Habtamu Tikubet	_____	_____
	Internal examiner	Signature	Date
3.	Ato Tsegaye Feleke	_____	_____
	External examiner	Signature	Date
4.	Dr. Birhanu Besha	_____	_____
	Railway Center head	Signature	Date

ACKNOWLEDGEMENTS

First I would like to express my heart felt appreciation and gratitude to my advisor,Tollossa Deberie for his helpful advice and for the faith, guidance, and help that he gave to me during my project work to be completed. I would also like to thank him for giving me the idea to take the project and "run with it" which allowed me to enjoy the project that much more. Without these ideas, this project would not have been the success that it has become and he deserves the credit for originating the concepts.

I would like to thank all those individuals at Addis Ababa University who have Supported me throughout my time as a post graduate student. I would like to express my sincere gratitude to my examiner Ato Tsegaye, who placed his faith and guidance in me and encouraged me to work hard throughout this process and Ato Habtamu, who helps me and guide me in my research process.

I would also like to thank my classmates for their support, direction, and wonderful explanations to help me further understand the basics of my research; and for their many recommendations and always helping me in idea as well as how to use the software's that helped me in doing the research

I would also like to express my gratitude to friends in Ethiopian rail way corporation, who Provided their vast knowledge of railroad design to help me complete this research.

I would like to thank my parents and step-parents for encouraging me in all of my endeavors. They have supported me emotionally and monetarily for many years. I would also like to thank my entire family, who have motivated me to aspire to higher education. They have all known when to push, when to hold my hand, when to send a smile, and when to let go.

I would also like to thank Ato Yusuf, Ethiopian railway corporation human power manager who provided support and help in obtaining data, from someone who has vast knowledge of the railroad industry and what it takes for a project to be successful. I would also like to give thanks to Ato Tekola, Ethiopian railway corporation vice manager for his help on this project.

ABSTRACT

The goal of this study is analyzing and identifying the stresses on bolted rail joint due to the wheel load to predict and minimize failures caused. The three dimensional model has been developed on modeling package of CATIAV5R16. In CATIAV5R16, different components of wheel/rail assembly i.e. wheel, rail, joint, bars, nuts, bolts are created separately then all components are assembled, and create a complete model of wheel/rail assembly. Assembly model has created in assemble workbench of CATIA after individual component of joint had created on part work bench. After the assembly is accomplished on CATIA, it was imported in to the ANSYS v14.5 to analyze the stress caused by vertical load. The material properties of the rail and wheel are assumed to be same. All the material properties and boundary conditions are being applied to estimate fatigue stress. The analysis using the software ANSYS includes fatigue stress, fatigue life, von miss stresses, shear stress and Equivalent elastic strain. These values have been determined under the influence of axle load. The result obtained in this analysis is better stress values for rail joint assembled by the modified geometry than the existing joint bar. During the rail joint analysis Joint between the sleepers needed more attention than other parts, to reduce the problem related to the rail joint.

Key Words: Rail Joint, Modeling, Finite Element Method

Table of Content

LIST OF TABLE

LIST OF FIGURE

NOMENCLATURE

a: Minor semi axes of the contact ellipse

b: Major semi axes of the contact ellipse

F: Vertical load, JBG:joint bar geometry

m & n :Hertz coefficients

Kw: Constants that depend on the material properties of railway wheel

ν_w: Poisson's ratio wheel material

E_w: Young's modulus of the railway wheel material

ν_r: Poisson's ratio of rail material

E_r: Young's modulus of rail material

R_{1w}: Principal rolling radii of the wheel

R_{1r}: Principal rolling radii of rail

R_{2w}: Principal transverese radii of curvature of wheel

R_{2r}: Principal transverese radii of curvature of radii

K : Stiffness matrix of the system

U: Nodal displacement vector

Γ_1: Boundary with zero displacement,

$\Gamma_{2:}$ Boundary where measured displacements are given

Γ_3: Boundary with unknown contact forces F_c

$\Gamma_{4:}$ Boundary where there are known applied forces

F_a: Applied forces

U_1: Displacements on constrained boundary Γ_1

$U_{2:}$ Known and measured displacements on free boundary Γ_2

U_3: Unknown displacements on contact boundary Γ_3

U_4: Unknown displacements on boundary Γ_4

σ : Stress vector, EFA: Finite Element Analysis

D: Elastic stiffness matrix.

$\in^{el}$: Strain that cause stress

$E_{x:}$ Young's modulus in the x direction

Gxy: Shear modulus in the xy plane

Vxy: Major poison's ratio

$v_{yx:}$ Minor poison's

σ_x: Stress in x direction

σ_y: Stress in y direction

σ_z: Stress in z direction

σ_{xc}^{f}: Normal stress failure in x direction

σ_{yc}^{f}: Normal stress failure in y direction

σ_{zyc}^{f}: Normal stress failure in z direction

σ_{xy}: Shear failure in xy direction

σ_{xy}: Shear failure in yz direction

σ_{xy}: Shear failure in xz direction

LRT: Light rail transit

RJ: Rail joint

CWR: continuous welded rail

IRJ: Insulated Rail Joint

FEM: Finite Element Method

CHAPTER ONE

INTRODUCTION

1.1. Background

A rail joint is the weakest link in the track. There is a break in the continuity of the rail in horizontal as well as in vertical plane at this location because of the expansion gap and imperfection in the rail heads at joint. The fitting at the joint become loose, causing heavy wear and tear to the track materials. There are essentially three different types of rail joints:

- Bolted joints
- Compromise joints
- Insulated joints

Bolted joints are used to join two rails in jointed rail territory. In continuous welded rail (CWR) where rails are continuously jointed in a territory, bolted joints are used to temporarily join rails before they are welded. Compromise bars are used to join two rails with differing sections. Insulated joints are further categorized as bonded or no bonded joints. Bonded insulated joints are glued. No bonded insulated joints are basically bolted joints having some type of electrical insulating properties [38].

The bolted rail joint in service today in CWR territory is essentially the same joint that was designed in the early part of the last century to provide vertical and horizontal rail alignment but allow longitudinal movement to offset rail expansion and contraction due to temperature change. While the shapes of the joint bars have changed to better match the heavier rails now in service, the joint is still designed to minimize the contact area between the joint bar and the rail web in order to accommodate longitudinal rail movement. Their function is to electrically connect two sections of a track from each other. The sectioning is utilized for signaling purposes: When a train operates on a track section it's wheel set will short-circuit the rails. If it can be identified which track section that is short-circuited the position of the train is known. Insulating joints can be designed in different ways. A normal configuration is that the rail is cut transversally and an insulated polymer layer is placed (glued) in the gap between the rail ends. The joint is assembled using two beams (fishplates) that are bolted to each side of the rail. The joint is often prefabricated and the joint section assembled in the track by bolting. The running surface was provided with an uprising edge in order to keep the vehicles on the track. Due to increasing of

iron production in England in 1760, the wooden rails were covered with cast iron plates, which caused the running resistance to diminish to such an extent that the application of such plates soon proliferated. About 1800 the first free bearing rails were applied which were supported at the ends by cast iron sockets on wooden sleepers.

1.1.1. History of the rail joint

Insulating joints are weak points of the rail that frequently cause problems. This can be attributed to the mechanical characteristics of an insulated joint. The joint imposes a sudden variation in track stiffness due to the change in bending and shear stiffness of the rail and the added weight of the fishplates. Further wheel– rail impact loads are often generated at insulated joints because of a local rail surface irregularity caused by misalignment and plastic deformations of the rail ends, [23]. In addition, the insulating layer is very flexible in comparison to the rail. In practice the insulating gap can therefore be considered as a free end of the rail. This results in a severe stress concentration at the insulating layer.

Figure 1.1 A newly installed insulated joint on The West Coast Line in Sweden [23]

A fundamental question in the study of mechanical deterioration of insulated joints is whether an increased joint gap will alleviate or aggravate the problem with deteriorated insulated joints. That the answer is not straight forward is indicated by the fact that joint gaps currently adopted vary. In order to answer this question more in-depth knowledge on the consequences of altered insulating gaps is needed. To this end, a detailed study of the deterioration of the rail material in the joint close to the insulating layer is performed. There the material accumulates plastic

deformations, which leads to material failure causing chips of metal to break off. This may result in the formation of an electrically conductive bridge over the insulating layer,

Causing malfunction of the signalling system. In Figure 1.2 deteriorated insulated joint is shown. Other failure modes for insulated joints include run-down of the joints resulting in a dipped joint that will cause high vertical load magnitudes and subsequent secondary damages. Also formation of corrugation and squats are rather common in the vicinity of an insulated joint due to the non-continuous track stiffness at the joint.

Figure 1.2: deteriorated insulated joint [24] and [25]

According to FRA's accident data, a total of 242 accidents related to joint failures occurred from 2000 to 2009 (Figure 1.3). Most joint bar failures occurred due to cracks initiated from bolt holes or at the bottom or top edges of the joint bars. The number of accidents caused by joint bars was relatively consistent until 2007. The sharp decrease observed in 2008 and 2009 appears to be due to lower traffic and the overall downward industry trend in accidents. Rail joints are typically not one of the five leading track causes of accidents in the FRA accident database. However, the industry is experiencing some joint caused accidents.

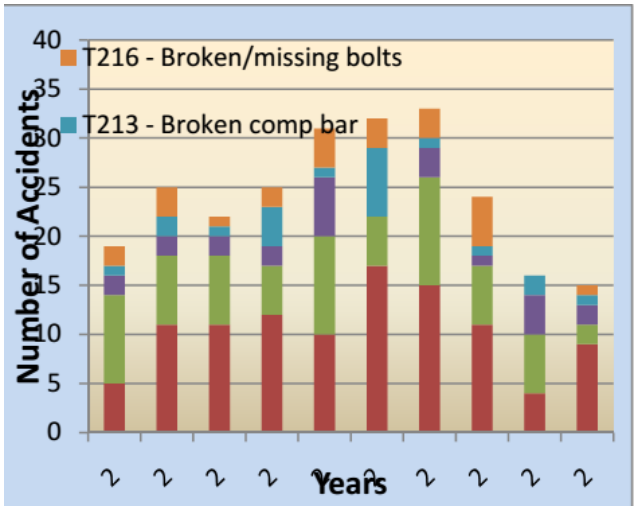

Figure 1.3. Joint bar related accidents by year, joint type, and failure mode [26]

The joint bar IJs are subjected to a number of loading scenarios in the field. Their ability to withstand these loads will determine their service life. At any given instance, only one wheel can be located within the span of a sleeper as the sleeper spacing is kept smaller than the wheel set spacing in the bogie structure. Therefore, an examination of the behavior of IRJs (either suspended between sleepers or supported on a sleeper) is essential to understanding of their performance. Figure 1.4 illustrates the deformation of a suspended and a supported IRJ when subjected to wheel loading.

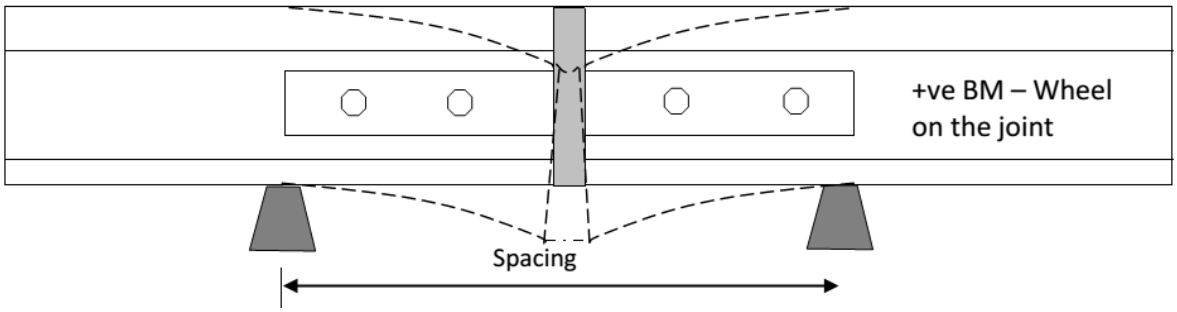

Figure1.4: Behaviors of suspended (top) and supported (bottom) IRJs in response to wheel loading. It is clear that edge of a rail end (point of stress concentration zones/ singularities) on a supported joint is more vulnerable to direct impact from the running wheels. Limited finite element (FE) studies by [17] confirm that supported joints exhibit higher impact than their suspended counterparts.

Many Commercial Vehicles also use bolted rail joint, although their exposed nature can present problems in certain heavy duty environments. In addition many locomotives and rolling stock utilize bolted rail joint.

1.1.2. Failure Modes

As highlighted in this report, IRJs fail due to a range of mechanisms. Each component that forms the IRJ (including interfaces between these components) fail under severe wheel-rail contact impact loading. Examples of some of the major failure modes of IRjs reported in the literature are shown in Figure1.5.

(a) Rail end battering

(b) Rail end shelling

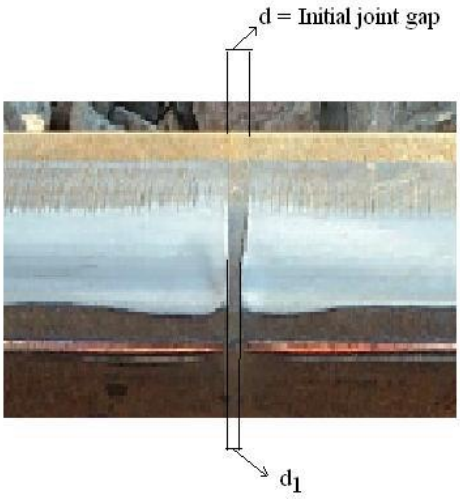

(c) Rail end metal flow

(d) Endpost battering/ delamination

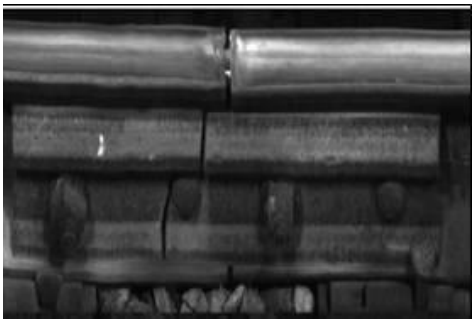

(e) Cracked joint bar

(f) Railhead spalling

(g) Chipping at rail end and gage corner

(h) Railhead crushing

(i) Typical pull-apart of IRJ in track

(j) Dipping of IRJ in track

Figure 1.5: The most common failure modes of rail joints reported in the literature: (a)–(j).[27]

Joints with complete epoxy failure are subject to all of the problems described above for bolted joints, such as wide rail gaps, broken track bolts, and bolt-hole cracks. In fact, they may be weaker than a conventional bolted joint, because the shape of the joint bar is optimized for maximizing the bond surface rather than for sustaining contact loads.

1.1.3. Rail Length

Rail is manufactured in different length as the mill the country has. Rail length increase over the years to prevent damage related to joint of the rail by avoiding the discontinuous between the rails. The rail length increases from 11.8 meter to 25meter. In some country, they can produce at 122meter length of rail. Nowadays, different countries use 25m of rail commonly including Ethiopia. These extremely long rails were developed in response to reducing the number of rail joint necessary to produce continuous series of rail. However, extremely long rails require special handling methods and equipment so that to avoid damage and obviously cannot be routinely moved over the highway. Such lengths of rail should favorable conditions for delivery and handling.

1.1.4. Joining Rails

Rails are produce in fixed lengths and need to be joined end-to-end to make a continuous surface on which trains may run. There are essentially two different type of a rail joint.

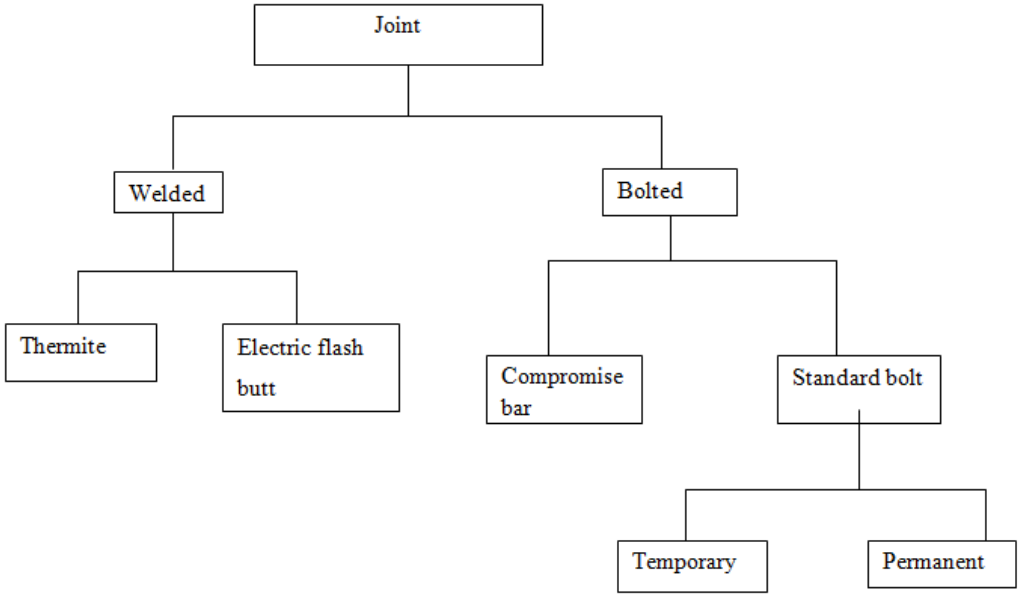

Figure 1.6: Rail joint classification

I. Welded joint

In this form of track, the rails are welded together by utilizing flash butt welding to form one continuous rail that may be several kilometers long, or thermite welding to repair or splice together existing CWR segments. This form of track is strong, gives a smooth ride and needs less maintenance. The trains can travel on it at higher speeds and with less friction.

Welded rails are more expensive to lay than jointed tracks, but have much lower maintenance costs. The first welded track was used in Germany at 1924 and in US at 1930, and it has become common on main lines since the 1950s [28]. There are two common types of rail welding:

- Exothermic ("Thermite") Rail Welding

Thermite welds are produced with molten steel cast from a crucible and poured into a specified gap between two rails. The molten steel is produced by an "exothermic" chemical reaction between aluminum and iron oxides. Additives in the mix create the other components needed to make the steel. Thermite welding requires preheating the rail ends in order to create a good bond between the rail steel and new steel produced in the thermite crucible. It is desirable that the resultant steel weld material have approximately the same hardness as the parent rail steel. Manufacturers can produce welds with different hardness's to provide compatibility with different grades of rail steel.

II. Bolted joint

The purposes of the rail joint are to hold the two ends of the rail in place and act as a bridge between the rail ends. The joint bars prevent lateral or vertical movement of the rail ends and permit the longitudinal movement of the rails for expanding or contracting. The rail joint is considered the weakest part of the track structure and should be eliminated wherever possible. Joint bars are matched to the appropriate rail section. Each rail section has a designated drilling pattern (spacing of holes from the end of the rail as well as dimension above the base) that must be matched by the joint bars. Although many sections utilize the same whole spacing and are even close with regard to web height, it is essential that the right bars are used so that joint bar angles and radii are matched. Failure to do so will result in an inadequately supported joint and will promote rail defects such as head and web separations and bolt hole breaks [29].

There are three basic types of rail joints:

- Standard(non- insulated) rail joint

Standard joint bars connect two rails of the same weight and section. They are typically 610mm in length with 4-bolt holes for the smaller rail sections or 940mm length with 6-bolt holes for the larger rail sections. Alternate holes are elliptical in punching to accommodate the oval necked track bolt. The standard joint consists: joint bar bolt with nut, washer and joint bar.
Insulated rail joints (IRJ's) are the epoxy binds the joint bars to the rails and allows very little relative movement and is widely used throughout the North American rail network.
Most mainline track uses "bonded" or "glued" IJ's in which the insulator separating the joint bars from the rails is embedded in a strong epoxy [37]

1.1.5 Joint Bars

While joint bar design has remained relatively unchanged for many years, recent industry research and development activity for bonded insulated joints has resulted in significant improvements in the performance of these components over the past 10 years. Some of these improvements can also be applied to standard (none insulated) rail joints. Current joint bar designs originated when most track was comprised of jointed rail. The bars were developed to allow relative movement (with respect to each other) of the rails in a joint. Joint bar used to connect the two rails together with fish bolt. There are different types of joint bars and some of them are currently in service.

- Splice
- Full toe
- Short toe

This research uses the modified short toe joint bar to entire study to analysis the joint bar stresses.

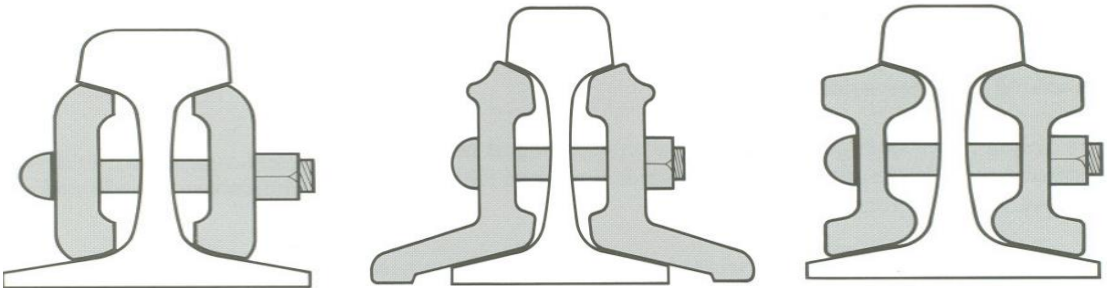

a. Splice b. Full Toe c. Short Toe

Other types of joint bars

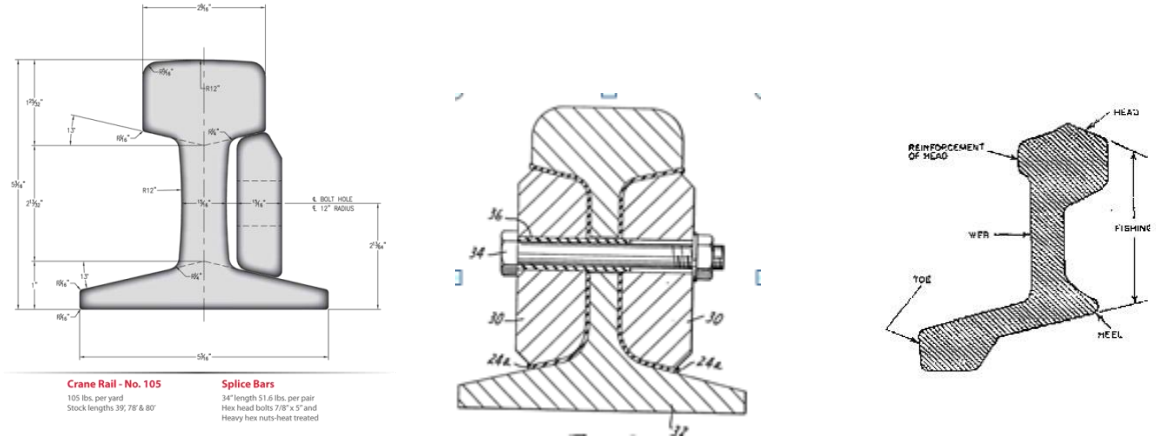

Figure 1.7: Type of rail joint bars [30]

Cross sectional area for the most commonly used joint bars are shown below.

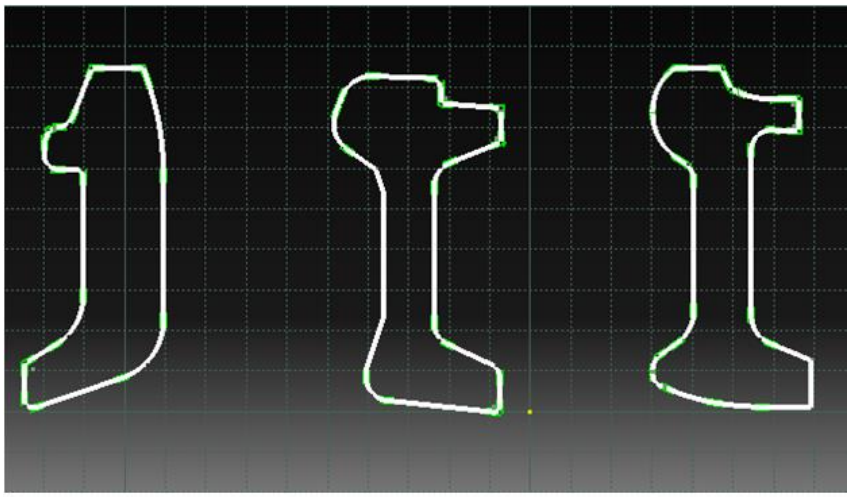

Figure 1.8: geometry for the commonly used rail joint bars [31]

Table 1.1 cross sectional areas for the mostly used joint bar [31]

Joint bar type	Cross-sectional area(in^2)
(a) IJ	6.27
(b) Short Toe	5.89
(c) High relief	5.64

The shape of the joint bar largely depends on its intended usage

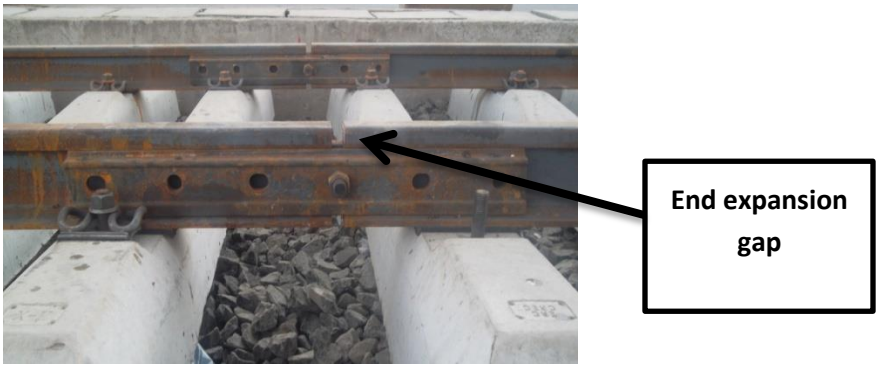

Figure 1.9: Standard rail joint of Ethiopia LRT. [32]

1.2 Statement of the problem

By their very nature, rail joints create discontinuities in the running surface of the rails. In addition to bending, residual stresses, rail joints are also subjected to static load due to these discontinuities. Under normal track and load conditions, joint bars fail due to high cycle fatigue, which is evident from fatigue striations observed on broken bars. Accelerated track degradation increases deflections, which further increase joint bar stresses, possibly changing the failure from high cycle fatigue to low cycle fatigue and in some cases even yielding. The current joint bar design is meant to support only the railhead and base. This feature is of limited value in continuous welded rail (CWR) where resistance to longitudinal force loads is also desired. Rail joint bar failures are a safety and reliability concern for railroads. Because of their redundancy (i.e. two bars in each joint), a failed joint bar is almost always found and replaced before an accident occurs. These stresses on the rail head produce the deflection on the joint that causes to vary on the rail and rail joint profile. As the result, the profile of rail joint component change from its normal profile it originates the discomfort and safety problem to the passenger and accident on the vehicle by causing wear on joint part identification and improving of the stresses on the rail joint assist to increase material property for rail joint, to reduce and avoid the discomfort of the passenger, rail joint wear and rail joint maintenance cost by using of different mechanism to decrease the fatigue stress on rail joint component.

This paper tries to address the following questions:

1. What types of stresses are inducing on the rail joint due to wheel load?
2. What are consequences of the stress on rail joint?
3. How can we reduce all these wheel load effects?

1.3 Objective of the Present Study

1.3.1 General Objective

The main objective of the study is analyzing and improving the stresses on rail joint due to the wheel load, which cause failure. The present investigation is aimed:

- To study fatigue stress analysis of the rail joint at straight rail joint conditions.

1.3.2 Specific Objective

The specific objective of the research is to:

- analyses the von miss stresses caused by wheel load
- Reduce the deformation on the rail joint.
- Determine strain, which generate stress on the joint.
- Reduce Fatigue stresses on the rail joint.
- Estimate fatigue life of the rail joint

1.4 Methodology of the Research

To fulfill the objectives of the study there are procedures that should be followed. The 3D model has done on modeling package of CATIAV5R16. Identify the rail joint used to connect the two end rail and Select the position of rail joint set between the ties. In CATIAV5R16, different components of wheel/rail assembly i.e. wheel, rail, joint, bars, nuts, bolts are created separately then all components are assembled, and create a complete model of wheel/rail assembly. Assembly model has created in assemble workbench of CATIA after individual component of joint had created on part work bench. One of the basic focus of this research is modifying the existing joint bar geometry by increasing the section area in CATIA work bench,JBG2 and the existing joint bar redrawn by CATIA workbench,JBG1[32].After the assembly is accomplished on CATIA, it was imported in to the ANSYS v14.5 to analyze the stress caused by vertical load. The meshing type for this research is medium size meshing. All the material properties and boundary conditions are being applied. During the analysis of wheel/rail contact in ANSYS software, the parameters have been used axle load, angular velocity and simulation result is obtained. The vertical wheel load is applied on the axle seat of the wheel.

1.5 Significance of the Research

This research has a great role for future analysis and uses of rail joint, in general for newly constructing Ethiopian railway by finding the new research. In the future, it will add new knowledge about existing one with analysis of rail joint stress, strain, deflection under vertical wheel load, which cause wear, fracture and deteriorations of the rail. This paper try to figure out those problems related to the rail joint due to the wheel load in between the sleeper supports based on engineering mechanics.

1.6 General Parameters and Conditions

1.6.1. General parameters

There are parameters to analyze the stress at the rail joint between the sleeper supports of the rail. These parameters can be classified as follows:

- Vehicle parameters: operating speed, Empty vehicle, Seating capacity and overload capacity
- Track parameters: Rail and joint bar profile, tie space and rail joint geometry (straight, location of rail between the tie).

1.6.2. General conditions

During the preparation of this paper the general conditions that have been using the effect of the wheel and rail contact at rail joint. It is performed based on the Hertz contact theory. These are:

- The surface of contacting bodies is assumed smooth.
- The contact is assumed elastic.
- Isotropic and homogeneous material.

1.7 Scope and Limit of the Thesis

As it can be seen, numerous types of simulations can be carried out regarding to railway track joint. In this research, as it is mentioned earlier, fatigue stress analysis of a rail joint structure are carried out. Nonlinear behavior which components could experience is not dealt with and, linear and isotropic material models are used for the entire analysis. In the static analysis, damping properties of the structures is not considered. The analysis is carried out only at the middle between the sleepers of rail joint. The effect of bolt torque and friction is not taken into account when the analysis preformed. This study is to reduce stress to succeed the rail joint. The limitations of the researches are lack of data, lack of high performance computer and lack of enough reference books to the research.

1.8 Organization of the Paper

The body of this study is divided into five main chapters. The first chapter discusses background, objectives and methodology of the study. In addition, the details of the rail joint type and rail joint used for analyze. The second chapter covers the review of some of the journal

articles, conference papers and publications which were referred to during the study. Also, in relation and comparison with previous works, what is done in this study will be stated. Analysis of stress on rail joint is discussed in the third chapter. Modeling contact at rail joint, stress model using hertzian theory, rail support and wheel rail simulation presented. In addition, it covers discretization of the solid model of the rail joint used for the analysis and load condition. The results obtained from the static and fatigue analysis of the rail joint and discussions based on these results are included in the fourth chapter. Finally, the fifth chapter cover conclusions drawn based on the results of the analysis, recommendations and future work.

CHAPTER TWO

2.1 REVIEW OF LITERATURE

2.1.1. Related Research

Fatigue life estimates can be used to guide the selection of inspection intervals for rail joint bars in service. A three -dimensional finite element model for rail joint bars is developed and dynamic load is applied to estimate the fatigue life of the joint bars. Different components of the rail joint bars are being created separately and assemble in ABAQUS. The model consists of assembly of the rail, joint bars, bolts, nuts, washers, and wheel. A three -dimensional finite element analysis of rail joint bars is carried out in ANSYS after importing from ABAQUS [34]

[1] Create relatively complex and realistic three-dimensional structures that can be analyzed much more quickly and still provide reasonable results for studying the effect of critical parameters. And puts some of the sections that describe the methodology behind the creation of rail elements for use in a standard joint model utilizing shell elements. This was performed in order to investigate the effectiveness of shells in modeling rail elements and to compare the results to the investigations by [1].

In the study [1] investigated a standard joint configuration connecting two sections of open track. A wheel load of 19958.064kg and a longitudinal thermal-induced load of 90718.474kg were used. Additionally, foundation stiffness's of 10342135.9397N/m^2 and 31026447.819N/m^2 were used for summer conditions and winter conditions, respectively. A tie spacing of 0.6096m was used but the tie width was not provided. The total length of the structure was 12.192m, in which two 240" pieces of rail were connected at the standard joint. Additionally [4] only considered the case where the ends of the rail are suspended by the rail ties at the connection. That is, there is no tie directly beneath the ends of each rail. The standard bolted joint relied on bearing on the joint bar / rail interface and the bolts to carry load across the joint [4]. On the other hand, the bonded insulated joint model transferred all load through the epoxy layer between the rail and joint bars [2]. The model created for the present study utilizes a combination of friction between the joint bar and rail, bearing between the joint bar and rail, and the bolted connection to resist the wheel load. Given the known limitations of the shell model and the differences between the

models, the results in were considered acceptable and the general behavior of the model matched expectations. The stress result is the von Miss stresses around the bolt holes of one of the rail segments when subjected to different combinations of longitudinal and vertical loading. In this case, the foundation stiffness was held constant at 20684271.84N/m^2 for each loading case to isolate the effect of the load on the response around the bolt holes. In the top image, a 2068427187.9535N/m^2 longitudinal load was applied at the end of each rail to simulate winter contraction of the rails. The bottom image shows the stress contours when the structure was subjected to the 224079612.0253N/m^2 wheel load only. It is apparent that the contribution of the longitudinal tensile load to the von Miss stress is significantly greater than the contribution from the vertical wheel load.

[4] Performed finite element analyses to examine the behavior of standard, bolted rail butt joints. They also performed finite element investigations into temporary joint-strengthening solutions and new joint designs. The goal of their research was to devise a new joint design that would improve the performance of bolted rail-rail joints in the field under ever-increasing axle loads. [4] Also used three-dimensional solid elements to create realistic models of the joint elements. Their analysis [1] considered both winter and summer conditions, particularly because a larger portion of joint failures occur during the winter [1]. In the winter, the foundation provides added stiffness but there is a large tensile, longitudinal load imposed on the joint due to the tendency of the rails to shrink under very cold temperatures. Their first study concluded that the standard joint used in practice for many years is structurally deficient for the current vertical loads.

[35]: Studied investigates an engineering analysis of different designs and failure modes of the IRJ by using a 3D finite element model for analyzing the stresses and strain on rail head. It was present a sensitivity analysis of different joint bar thicknesses (30mm, 34mm, and 40mm) to compare stress and strain distributions on the railhead. It was a small reduction in the stresses encountered by the rail when joined with a pair of joint bars of increased moment of inertia considering the thickness range considered. It suggests that increasing bending stiffness by increasing the thickness of the joint bar is not a good way to reduce stresses and displacements of the rail joint. An important way of increasing bending stiffness of the bar is to increase its height. The increase of stiffness of the bar by increasing height is more dominant compared to that of thickness.

[3] The response of the standard joint model under vertical loading is considered. The designed section considers the effects of mesh refinement on vertical deflection of the standard joint. The vertical deflection of one rail when using three different meshes. "Fine" refers to the mesh with the most elements, while "Coarse" refers to the least refined mesh. [3] beam on elastic foundation model for a piece of straight rail without a joint, the joint should deflect significantly more than the infinite beam under loading and the model results reflect this. Additionally, the mesh refinement results in very little improvement in the accuracy of the vertical deflection. Although the global deflection changed very little during mesh refinement, the finest mesh did result in some small improvements near the application of load.

[23] carried a numerical analysis combining dynamic and plastic deformation and material deterioration of IRJ's to investigate the influence of the rail joint on generation of wheel-rail impact load and subsequent material deterioration of the joint. It was argued that these joints form local irregularities and result in a local change of dynamic track stiffness. It was observed that not only the dynamic characteristics of the track by virtue of the presence of the IRJ were altered, but also the surface irregularities caused a high increase in contact load. Consequently, a high stress concentration and a corresponding plastic deformation occurred at the joint.

[5] Studied the stress around fish bolt hole by using static loading tests and field tests then compare to stresses were calculated by using FEM. Tensile stress field in the vertical direction occurred when joint bolts were fastened and the maximum stresses were generated at lateral positions of holes. Maximum stress amplitudes were observed at 45-degree position to longitudinal axis of rail under a vertical load. Based on results, they established a method to evaluate the stresses at the edges of fish bolt holes when fish bolts were fastened and trains passed.

[6] Studied change on insulated rail joint design in order to improve the performance of the insulated joint by using finite element method. ABAQUS software is used to model the supported butt joint. In this model, the rail, joint bars, epoxy, and ties surrounding the joint are modeled using solid elements. The remaining ties are modeled as an elastic foundation. The rail is subjected to a tensile load, as well as a vertical wheel load that is applied to the rail using Hertz contact theory. Parametric studies are performed by varying the tie width, joint bar length, and joint bar dimensions. Two different wheel load locations are also investigated: centered

about the end post, and halfway between the tie under the end post and the tie just to the left of the end post.

[7] studied the effects of epoxy deboning on the stress and strain are in a bonded insulated joint subjected to longitudinal force. Finite element method is used to model the different type of deboning feature. They studied the effect of the deboning by using ABAQUS software from their result; it shows under thermal tensile loads, strains at the center of the outer surface of the joint bar tend to increase as deboning begins near the end post. The strain at this point tends to stabilize after the deboning reaches the innermost bolt hole. Strain at a point between the outermost and middle bolt holes starts relatively stable, but increases after deboning passes the innermost bolt hole. From the standard joint model it was concluded that: the results from the shell element model matched the expected behavior of straight rail and a standard joint reasonably well, based on comparisons with prior numerical simulations and analytical beam on elastic foundation theory. As aforementioned rail joint is the weakest link in the track the components should be optimized by strong materials as well as parameter variation and to increase the bolt connection strength of the joint to have the best stress values.

[8] Is another relevant name in the study of dynamic loosening is, he was the first to study bleeding due to a transversal vibration. In addition, the testing machine he designed for conducting tests has become the typical device for testing joints under transversal vibrations. He stated, "Bolted connections loosen because the combined external force and circumferential component of the normal thread force overcome the friction forces holding the joints."

The Colorado-based Transportation Technology Centre, Inc. (TTCI) has been testing several IRJ (joints) prototypes in collaboration with the Association of American Railroads (AAR), the Federal Railroad Administration (FRA) and various rail industry organizations. These prototypes comprise new designs as well as modified versions of existing conventional joints. The focus of this collaborative design project is to develop stiffer and stronger joints that can withstand heavy axle loads without exhibiting any of the frequently observed failure mechanisms (i.e. adhesive deboning followed by joint bar cracking). [11–15]

[9] Carried out an analysis of insulated rail joints subjected to vertical wheel loads. They presented a semi-analytical relationship to illustrate bending moment distribution in the vicinity of joints and central deflections. It was indicated that the bending moment distribution leads to

delamination failure due to the large deflections at the joints. The most frequent cause of IJ insulation failure, as documented by the railroads, is adhesive debonding. The weakened adhesive bond allows moisture intrusion causing metal corrosion and adhesive deboning the higher stiffness of epoxy adhesives, as compared to the rail steel, seems to be responsible for cracks at the end post. In cases where most of the epoxy bond is still intact, shearing action in the bolts and friction at the deboned surfaces has little effect. On the other hand, when the epoxy deboning becomes extensive enough, the relative displacement between bars and rails grows larger. This allows the bars and rails to bear directly on the bolts, concentrating forces at the edges of the bolt holes. It also creates shear stress on the deboned surfaces that exceeds the maximum static friction stress and causes slippage

[10] In addition to bending, thermal, and residual stresses, rail joints are also subjected to dynamic loads due to these discontinuities. A lower difference in elastic modulus can reduce the interface stress magnitude in the rail ends; however, it could adversely result in higher stress in the insulation material, which may lead to its earlier failure. Electrical failure often results when the loose joint experiences contact between metal surfaces on the rails and joint bars or bolts – a result of fretting, deterioration or wear in the insulator, relative component movement, and related processes. According to FRA's accident data, a total of 242 accidents related to joint failures occurred from 2000 to 2009. Most joint bar failures occurred due to cracks initiated from bolt holes or at the bottom or top edges of the joint bars. The number of accidents caused by joint bars was relatively consistent until 2007. The sharp decrease observed in 2008 and 2009 appears to be due to lower traffic and the overall downward industry trend in accidents.

Bolted joints are used to join two rails in jointed rail territory. In continuous welded rail (CWR) territory, bolted joints are used to temporarily join rails before they are welded. Compromise bars are used to join two rails with differing sections. Insulated joints are further categorized as bonded or non-bonded joints. Bonded insulated joints are glued. Non bonded insulated joints are basically bolted joints having some type of electrical insulating properties. While these three types of rail joints perform differently and have different operational objectives, they share many similar design features. For example, they all use bolts and bars and create a discontinuity in the running surface of the rail. Bolts generally fail due to yielding, and bars usually fail due to fatigue. The discontinuity in the running surface of the rail creates conditions that can accelerate

track degradation around the joint. At a minimum, the gap at the rail ends within the rail joint is a source of impact loading from passing wheels. Left unchecked, these impact loads increase rail end batter, thereby deteriorating the foundations, which further increase the impact forces generated by passing wheels.

[15] Has studied that the finite element model for reverse bending calculates joint bar bending stresses that are comparable to the engineering estimates based on beam on elastic foundation theory. The engineering estimates are, therefore, an efficient method to estimate the tensile reverse bending stress at the top outer fiber of the joint bar, which is important for fatigue crack growth calculations. However, the finite element model for the wheel over the joint calculates stresses that are higher than the engineering approach.

Joint bar strength should be at least equal to the surrounding rail. Strength can be increased either by using higher strength materials or by increasing the cross section of joint bars. Joint bars have high residual stresses induced during manufacturing processes. Controlling residual stresses can be useful. Residual stresses should be tensile or compressive on joint bar locations where service loads induce compressive or tensile bending stresses respectively. This approach will not only increase joint bar load capacity, but also increase fatigue life. The shape of the joint bar largely depends on its intended usage

[16] research project, sponsored by the Federal Railroad Administration (FRA) has sponsored and managed research on safety matters related to railroad track and equipment for several decades rail integrity is an area of research under the FRA Track Safety Research Program, which deals with the prevention and control of rail failures. Rail failures, or broken rails, usually originate from defects that form and grow in the rail head as a result of metal fatigue. Past rail integrity research focused on defects that occur in continuous welded rail (CWR), primarily because of an increasing trend in the railroad industry to replace bolted joint rail . Rail joints, however, cannot be completely eliminated. For example, bolted joints are often used to connect strings of CWR. Bolted joints are also used for temporary repairs.

Observed problems from the study of surveyed Bars surveyed by FRA joint assemblies were identified as either a standard, compromise, or insulated bar [33]. Compromise joint bars are designed to join rail sections of different sizes while keeping the gage and running surfaces in

alignment. Insulated joint bars are needed where track circuits exist for signaling purposes. In addition, the surveyed bars were characterized as either angle, head-free, or head-contact bar (see Figure 2.1). Table 2.1 lists the number of failed or defective bars for these three different types found during the field surveys.

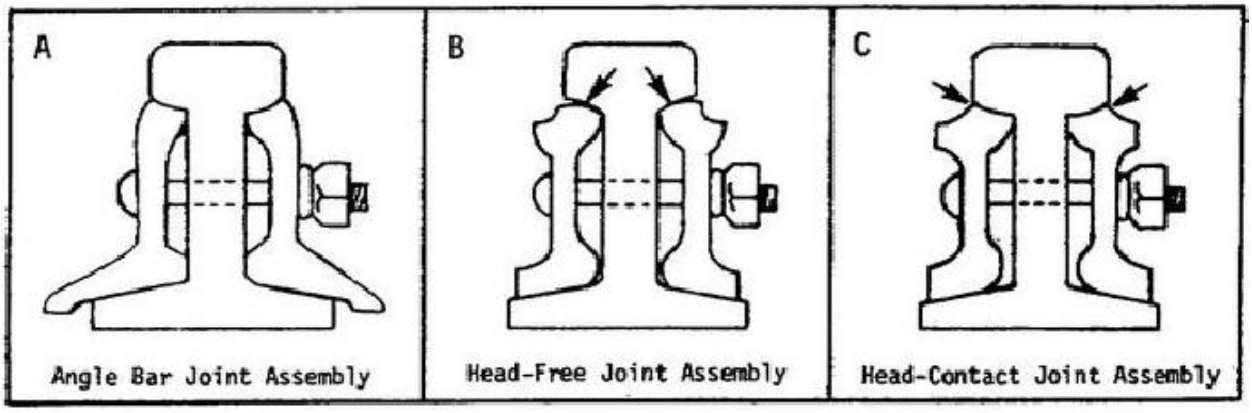

Figure 2.1: angle, head-free, or head-contact bar

Table 2.1: Composition of Defective Bars in Field Surveys

Type	Number of Defective Bars (% Total)
Long-Toe Angle Bar	47 (39%)
Head-Free Joint Bar	68 (56%)
Head-Contact Joint Bar	6 (5%)
TOTAL	121

From the above table the number of defective bars for the Head contact joint bar is small comparing to the others so that this joint bar is the main focus of the study [33].

2.1.2 Conclusions from Literature Review

The considerable numbers of problems caused by fatigue failure makes it an important point of research from economic and safety point of view. The engineering estimates are, therefore, an efficient method to estimate the tensile reverse bending stress at the top outer fiber of the joint

bar, which is important for fatigue crack growth calculations. However, the finite element model for the wheel over the joint calculates stresses that are higher than the engineering approach.

[15] The finite element model for reverse bending calculates joint bar bending stresses that are comparable to the engineering estimates based on beam on elastic foundation theory. The engineering estimates are, therefore, an efficient method to estimate the tensile reverse bending stress at the top outer fiber of the joint bar, which is important for fatigue crack growth calculations. However, the finite element model for the wheel over the joint calculates stresses that are higher than the engineering approach. Joint bar strength should be at least equal to the surrounding rail. Strength can be increased either by using higher strength materials or by increasing the cross section of joint bars.

In addition the related thesis studied in 2014 studies the stresses values in three cases: joint away from the sleeper, joint approaching to the sleeper and joint on the sleeper however the different stresses values are higher when the joint between the sleepers so that the main focus of the study in this research is when the joint between the sleepers by modifying the geometry of the joint bar.

CHAPTER THREE

MODEL AND FEA ANALYSIS OF STRAIGHT RAIL JOINT USING ANSYS

Most numerical approaches on rail joint indicated that a rail joint are the weakest link in the track. There is a break in the continuity of the rail in horizontal as well as in vertical plane at this location because of the expansion gap and Imperfection in the rail heads at joint. The fitting at the joint become loose, causing heavy wear and tear to the track materials. For analyzing the fatigue analysis, it is very useful to use FEM simulations based on the adopted analytical model for defining fatigue load sources at surfaces which are in contact with the joint.

This study will use the FEA software ANSYS14 version to carry out fatigue stress analysis and the mechanical stresses of a railway rail joint during wheel running conditions will be determined.

3.1 Introduction to Finite Element Analysis

Finite Element Method is a numerical procedure for solving continuum mechanics of problem with accuracy acceptable to engineers. Finite Element Method is a mathematical modeling tool involving discretization of a continuous domain using building-block entities called finite elements connected to each other by nodes for once and moment transfer. This process includes Finite Element Modeling and Finite Element Analysis.

In displacement based FEM, stiffness of the entire structure (Part or assembly) is assembled from stiffness of individual elements. Loads and boundary conditions are applied at the nodes and the resulting sets of the simultaneous equations are solved using matrix methods and numerical techniques. In short, FEM is a numerical method to solve ordinary differential equations of equilibrium. Starting with simple linear static stress and heat transfer analysis, complex simulations involving highly non-linear, fluid flow and dynamic events can be successfully analyzed on a personal computer using a host of popular software like ANSYS. In practice, a finite element analysis usually consists of three principal steps.

Preprocessing: Create and discretize the solution domain into finite elements. This involves dividing the domain into sub-domains, called 'elements', and selecting points, called nodes, on the inter-element boundaries or in the interior of the elements. Assume a function to represent the behavior of the element. This function is approximate and continuous and is called the "shape

function". Function". Develop equations for an element. Assemble the elements to represent the complete problem. Apply boundary conditions, initial conditions, and the loading.

Analysis: Solve a set of linear or nonlinear algebraic equations simultaneously to obtain nodal results, such as displacement values, or temperature values, depending on the type of problem.

3.2 Rail

Rails support and guide the wheels of the train vehicles. Rail profile has been the object of continuous improvement since the beginning of railways. The cross-sections of gauge rails have been standardized by the UIC.

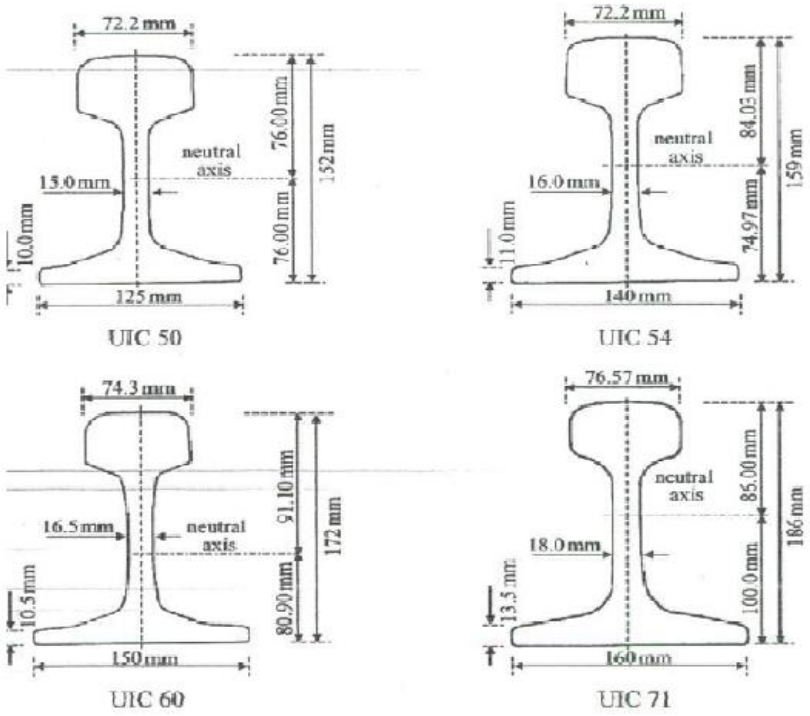

Figure 3.1: Rail profiles UIC 50 (50 E1), UIC 54 (54 E1), UIC 60 (60 E1) and UIC 71 (71 E1) [36]

Uic50 has been chosen to design and analyze. At first we notice the sizes offered by Vossloh conifer's company, these sizes have been shown in the table below:

Table3.1: The parameters of used rail uic50.

Parameters.	Dimensions in(mm)
The overall height of the rail	152
The width of rail	125
The height of railhead	49.4
The width of railhead	72.2

The rail is designed as a beam with the cross section of a UIC 50kg/m standard rail which is presented in Figure 3.2.Because the rail is interacting with wheel and transfers the sleepers, it remains the real cross section profile with exact dimensions, in order to keep the accuracy of the results.

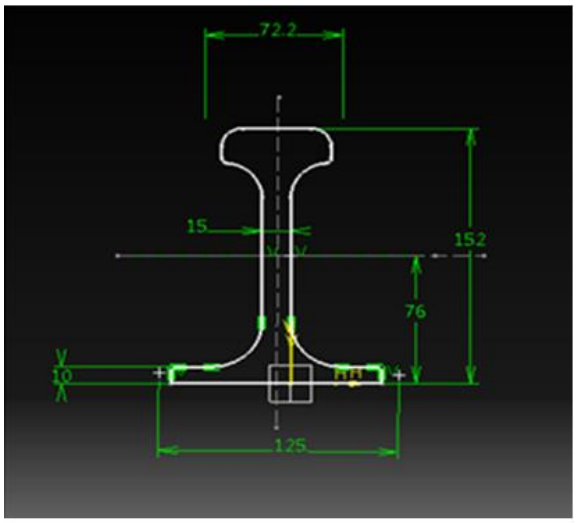

UIC50

Figure 3.2: Cross section of 50kg/m standard rail [36]

Rails are produced in fixed lengths and need to be joined end-to-end to make a continuous surface on which trains may run. However, presence of the joint caused the high stress on the rail, which produces the diverse type of wear at the rail head. This paper concerns on the stress distribution on rail joint under vertical wheel load.

Table 3.2: Dimensions and Specification

Item No	Technical parameters	values
1	Type of rails for main lines and depot	50 kg/m
2	Track gauge:	1435 mm
3	Wheel diameter (new wheel)	≤660 mm
4	Plate length	820 mm
5	Plate thickness	19 mm
6	Sleeper space	625 mm
7	End gap	5 mm
8	Joint bar bolt and nut	M28(AT109)
9	Spring washer	Φ34mm
10	Cross sectional area of rail	64.16cm2
11	Height of the rail	152mm
12	Length of the rail	25m
13	Tram car length	28400mm

3.2.1 Assumptions

- Material properties are isotropic and independent of the temperature;
- The nominal surface of contact between the rail joint and the wheel in operation is equal to the apparent surface in the sliding motion.
- The contact pressure distributed over friction surfaces is considered as symmetric.
- The average of the intensity of force into rail joint on the contact area equals.
- The surface of contacting bodies is assumed smooth.
- The wear on the contact surface is negligible.
- The effect of the load is not affected by season.

3.3 Joint bar

From [31] the most used joint bars; the cross section of short toe bar is changed. It is chosen since the surveyed bars were characterized as either angle, head-free, or head-contact bar (see Figure 2.1). Table 2.1 lists the number of failed or defective bars for these three different types found during the field surveys is short toe bar.

According to the study a Head-free bar which is the short toe bar was the most common design found during the surveys [31] and research on Stress Analysis of Rail Joint under Wheel Load [32], the short toe bar is chosen. When they are installed, head-free joint bars contact the rail at a single point in the head-web fillet region and the rail base. Head-contact joint bars are in full contact at the bottom of the rail head. Head-contact joint bars are assumed to promote rail failures by head-web separation, but are also claimed to provide additional stiffening for better ride quality. Therefor development is done on the head contact joint bar which is the short toe bar. The cross section of the short toe bar is 3799.9924mm2 depicted on table 1.1.

Table 3.3 shows overall dimensions of the JBG1and JBG2 bars.

	h(mm)	b(mm)	Easement region of the bar(mm)		Easement region Of the uic50 rail (mm)	
			Top	bottom	Top	bottom
JBG1	121	53	R22	R20	R22	R20
JBG2	121	53.8	R22	R20	R22	R20

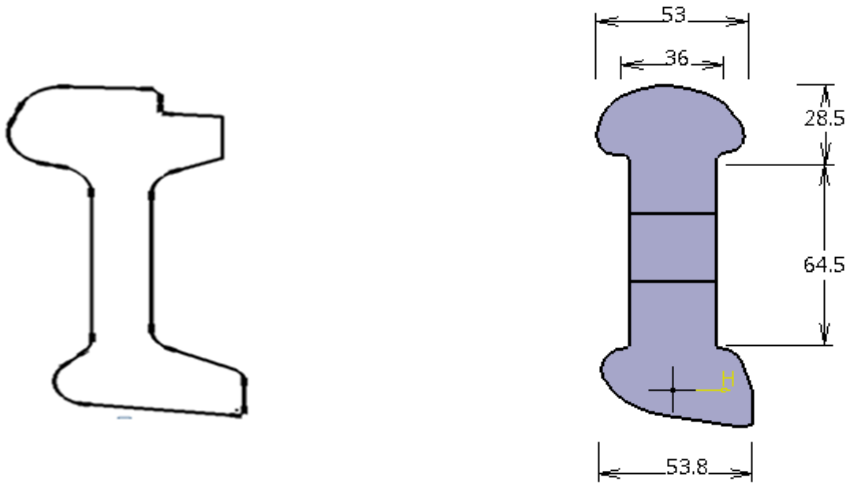

Figure 3.3: a) Short toe joint bar (JBG1) [31] b) the modified short toe joint bar (JBG2)

Cross sectional area for the short toe joint bar is

$5.89in^2=0.0037999924m^2=3799.9924mm^2$

But the cross sectional area for the bar developed is approximately $4374mm^2 = 6.779in^2$

3.4 Model and analysis of rail

Fatigue life estimates can be used to guide the selection of inspection intervals for rail joint bars in service. A three-dimensional finite element model for rail joint bars is developed and static load is applied to estimate the fatigue life of the joint bars. Different components of the rail joint bars are being created separately and assemble in CATIA. The model consists of assembly of the rail, joint bars, bolts, nuts, washers, and wheel. A three-dimensional finite element analysis of rail joint bars is carried out in ANSYS after importing from CATIA.

Surfaces of engineering components are consistently subjected to contact, thermal and others loading due to these large stresses applied over localized area. Many researchers studied different parameters and their influence to improve the failurities of the different component of the contact area.

There are different theories, analytical, numerical formula and finite element method developed in different time to solve the problem related to contact component and to increase the performance of the contact area. Although, railway systems are a transportation system still now it has a large number of unsolved problems that related to contact surface.

There are many theories on the contact geometry. However, many published papers use the hertz theory to understand it easily. The hertz theory has been developing since [22]Hertzian contact theory, explain a relationship for determining the contact pressure distribution and contact area of a solid bodies while in contact with an elastic sphere or cylinder under an applied load. This theory has its own assumption to solve the contact area and stress distribution of two solid bodies.

The following are the hertz theory assumption:-

- The contact between elastic bodies should be frictionless.
- The significant dimensions of the contact area should be much smaller than the dimensions and the radii of curvature of the bodies in contact.
- The contact between elastic bodies should be described by second-order polynomials.

The hertz theory has different type of contact for different shape of the solid body contact. The contact between the wheel/rail is elliptical contact. For wheel/rail contact hertz theory is much preferable than others theory.

The analysis of the wheel/rail contact is covered by using the elliptical contact shape to solve the stress, strain, deformation and fatigue life caused by the vertical load.

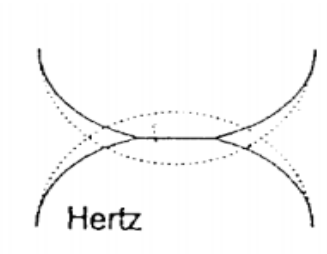

Figure 3.4: Full elastic contact mechanics model of hertz [17].

3.4.1Modeling Contact at Rail Joint

The wheel profile consists of a flange to guide the trains along the rails and a conical tread that contacts rail head, and rail has many curvatures to guide wheel properly. The contact positions of the wheel / rail are different in the different situation. However, this paper uses the contact between the wheels tread and rail head.

The contact area between wheel and rail are very small compared to their dimension.

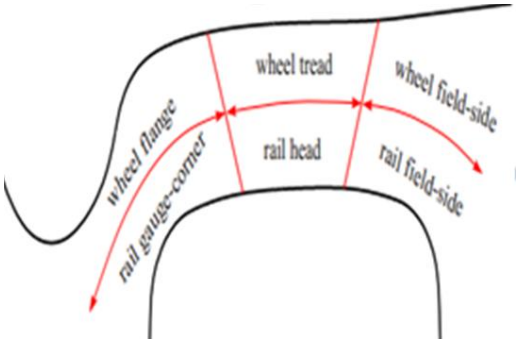

Figure 3.5: Contact zone of wheel/rail.

3.4.2 Stress Model Using Hertzian Theory

High stresses are inducing when a vertical load applied on the rail joint. This can cause serious problem on rail joint. Hertz developed a theory to calculate the contact area and stress between the two contact surfaces. The purpose of this paper is to focus on the hertz theory, when the wheel and rail contact occur at the end gap of the rail, however the contact is not a full contact due to the end gap. As shown in the figure below the joint bars are connected at rail web, so that the wheel doesn't contact to the joint bar

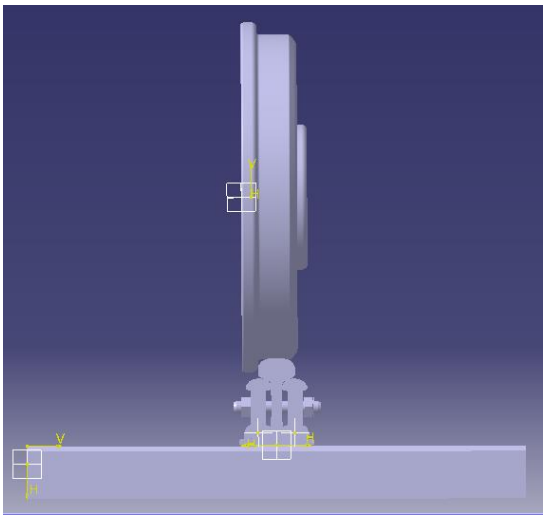

Figure3.6: Wheel/rail contact at rail joint.

3.4.3Wheel/rail Contact Mechanics

Surfaces of engineering components are routinely subjected to contact loading, where large stresses are applied over highly localized area. Many researchers have studied different parameters and their influence on the dynamic behavior of rotational system.

The stress field created by the contact stresses was first introduced by [39] Assessment of contact stresses at the wheel–rail interface is one of the most important aspects of railway research, considering the many phenomena involved. For this reason, many scientists have approached the problem mainly by means of theoretical or numerical solutions based on the Hertz's theory, which can be considered the basic starting point for all subsequent research. However, there are limiting conditions for the applications of the Hertz contact theory:

i. The contact between elastic bodies should be frictionless,
ii. The significant dimensions of the contact area should be much smaller than the dimensions and the radii of curvature of the bodies in contact.
iii. The contact between elastic bodies should be described by second-order polynomials.
iv. An elliptical contact area and an ellipsoidal normal contact pressure distribution are created at contact of the wheel and rail.

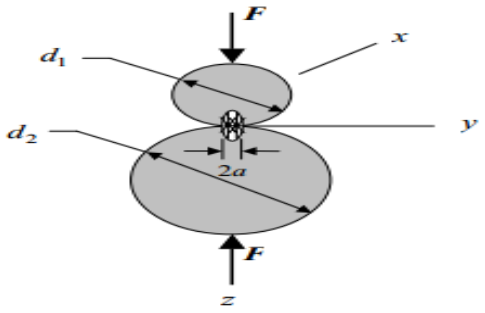

Figure3.7: An elliptical shape of contact stresses [40].

Due the above reason hertz's theory applied only for the straight surface and smooth it is not applied on the roughness and joint part of the rail head. Other method need to analysis the rough surface and join part of the rail head. Researcher also used different mechanism to deal the interaction between the wheel and rail.

When two elastic non-conforming bodies get together, according to the Hertz contact theory, the contact area is elliptical in shape with a major semi-axis "a" and a minor semi-axis "b"

The contact pressure distribution in this area represents as semi-ellipsoid, which can be expressed as:

$$P(r) = p_o \sqrt{1 - \frac{x^2}{a^2} - \frac{y^2}{b^2}} \quad \text{.....3.1}$$

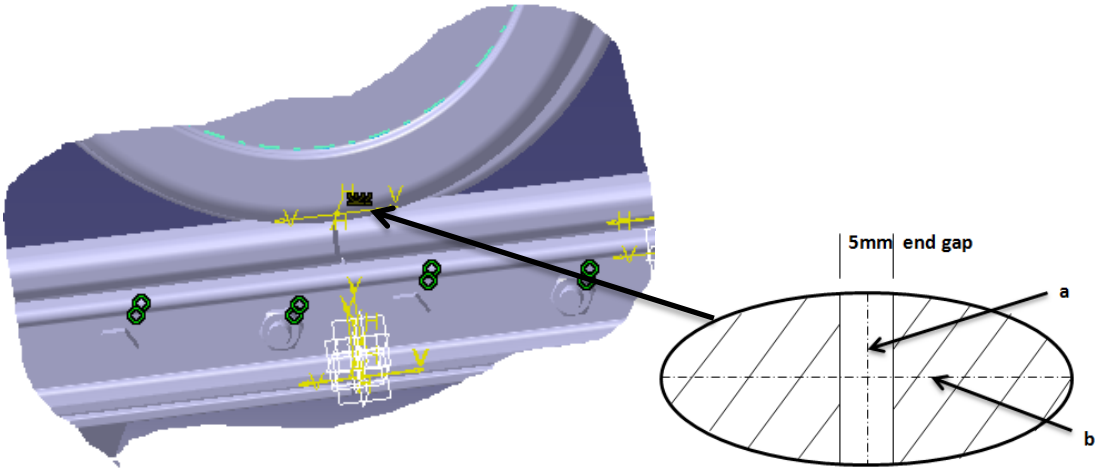

Figure 3.8: Shape of wheel/rail contact

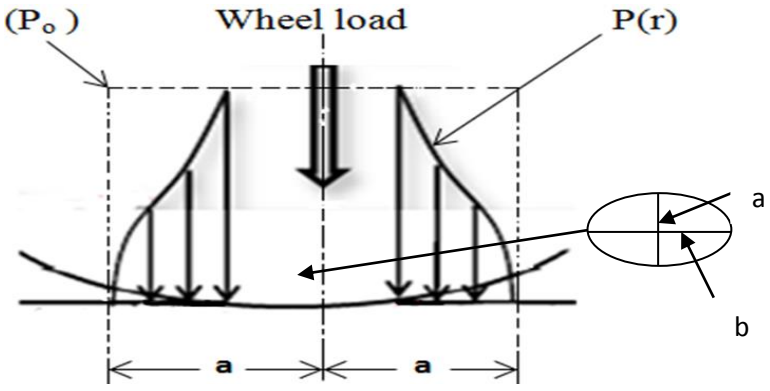

Figure3.9: Pressure distribution at contact zone of rail joint [18a].

Based on the Hertz contact theory, the contact point is very small relative to the overall dimension of wheel and rail surfaces. This very small contact point has elliptical shape. There is small gap on the pressure distribution due to the end gap on the joint.

From the above formula a and b are semi axes of the contact ellipse whereas x and y are the required coordinates to specify the point of contacts on the rail head based on the lateral rail surface parameter.

If x=0 and y=0 the point of contact is on the centerline of the rail head the stress is maximum,which is equal to:

P = p_o , where $p_o = \frac{3F}{2\pi\, ab}$ ……..…… 3.2

F is the vertical load act on the rail head

Based on the size and orientation of the contact, the positions of the contact point may be shifted in different directions based on the direction of x or y. However, based on Hertz contact formula and assumptions, the stress due to wheel/rail contact decreases and becomes zero when it goes far away from the centerline of the rail head. Similarly, the wheel/rail contact stress is inversely proportional to the major and minor axis of the contact ellipse[19].

The contact area determined as follows:

$$a = m\left(3\pi F\left(\frac{K_w + K_r}{4K_3}\right)\right)^{1/3} \quad \text{3.3}$$

$$b = n\left(3\pi F\left(\frac{K_w + K_r}{4K_3}\right)\right)^{1/3} \quad \text{3.4}$$

m and n are Hertz coefficients and they are given as a function of the angle (0^o -180^o)

$$\theta = \cos^{-1}\frac{K_4}{K_3} \quad \text{3.5}$$

θ is rail curvature

M,n are obtained by θ and from the table below:

Table 3.4: m,n quantities [20]

β	M	N
90	1	1
80	1.128	0.893
70	1.284	0.802
60	1.486	0.717
50	1.754	0.641
40	2.136	0.567
30	2.731	0.493
20	2.778	0.408
10	6.612	0.319

K_w and K_r are constants that depend on the material properties of railway wheel and rail respectively.

$$K_w = \frac{1-(\nu_w)^2}{\pi E_w} \quad \text{..... 3.6}$$

ν_w and E_w are Poisson's ratio and young's modulus of the railway wheel material respectively.

K_w is constants that depend on the material properties of railway wheel.

$$K_r = \frac{1-(\nu_r)^2}{\pi E_r} \quad \text{..... 3.7}$$

ν_r and E_r are Poisson's ratio and young's modulus of rail material

K_r is constants that depend on the material properties of rail.

$$K_3 = \frac{1}{2}\left(\frac{1}{R_{1w}} + \frac{1}{R_{2w}} + \frac{1}{R_{1r}} + \frac{1}{R_{2r}}\right), \quad \text{..... 3.8}$$

$$K_4 = \frac{1}{2}\left(\left(\frac{1}{R_{1w}} - \frac{1}{R_{2w}}\right)^2 + \left(\frac{1}{R_{1r}} + \frac{1}{R_{2r}}\right)^2 + 2\left(\frac{1}{R_{1w}} - \frac{1}{R_{2w}}\right)\left(\frac{1}{R_{1r}} - \frac{1}{R_{2r}}\right) cos2\varphi \right)^{1/2} \quad \text{.....3.9}$$

K_3 and K_4 are depends on the geometric propeties of the two bodies.

R_{1w} and R_{1r} are the principal rolling radii of the wheel and rail respectively.

R_{2w} and R_{2r} are the principal transverese radii of curvature of the wheel and radii respectively.

φ is straight segment curvature of the rail.

The direction of the axes of the contact ellipse can be determined based on the radii of curvature and the rolling radii for the two bodies in contact.

If $\frac{1}{R_{1w}} + \frac{1}{R_{2w}} \geq \frac{1}{R_{1r}} + \frac{1}{R_{2r}}$: the transverse semi axis of the contact ellipse (y direction) is greater than or equal to the longitudinal semi-aixs.

If $\frac{1}{R_{1w}} + \frac{1}{R_{2w}} \leq \frac{1}{R_{1r}} + \frac{1}{R_{2r}}$: the transverse semi axis of the contact ellipse (y direction) is less than or equal to the longitudinal semi-axis.

3.5 Finite Element Theory For Contact Body

Finite element theory is used to show that relationship among the contact force, applied force, support and free displacement of wheel /rail contact. During the formulations of finite element the contact between the wheel and rail is assumed:

- Isotropic
- Homogeneous
- Linear elastic body Ω with boundary conditions

The linear elastic bodies have four boundaries condition as shown in the figure below.

- Γ_1 is the boundary with zero displacement,
- Γ_2 is the boundary where measured displacements are given,

- Γ_3 is the boundary with unknown contact forces F_c and unknown contact deformation or displacements,
- Γ_4 is the boundary where applied forces F_a and the other are free surface except those mentioned above. The displacements on boundary $\Gamma_4$are unknown.

Let's recall the general form of static finite element system, which is

$$KU=F \text{ [18]} \qquad \ldots\ldots\ldots\ldots\ldots\ldots\ldots \quad 3.10$$

K, U and F are stiffness matrix of the system, nodal vector displacement, and nodal vector forces. According to the classification of the boundary, it constructs the finite element equation in the following form:

$$\begin{bmatrix} K_{11} & K_{12} & K_{13} & K_{14} \\ K_{21} & K_{22} & K_{23} & K_{24} \\ K_{31} & K_{32} & K_{33} & K_{34} \\ K_{41} & K_{42} & K_{43} & K_{44} \end{bmatrix} \begin{bmatrix} U_1 \\ U_2 \\ U_3 \\ U_4 \end{bmatrix} = \begin{bmatrix} F_1 \\ F_2 \\ F_3 \\ F_4 \end{bmatrix} \qquad \ldots\ldots\ldots 3.11$$

K_{ij} and $F_1$are sub-stiffness matrix, and vector of reaction forces on the boundary Γ_1.

$\overline{F}_2$ is a vector forces on the boundary Γ_2 with measured displacements, usually there is no force on the measured boundary.

F_c and F_a are vector of unknown reaction or contact forces on the boundary Γ_3 and vector of known applied forces on the boundary Γ_4.

$\overline{U}_1$ and U_2 are known displacements on constrained boundary $\Gamma_1$and measured displacement on free boundaryΓ_2

U_3 and U_4 are unknown displacements on contact boundary Γ_3 and unknown displacements on boundary Γ4with known applied force Fa, the free surface with no applied force and the internal nodes where net force is zero.

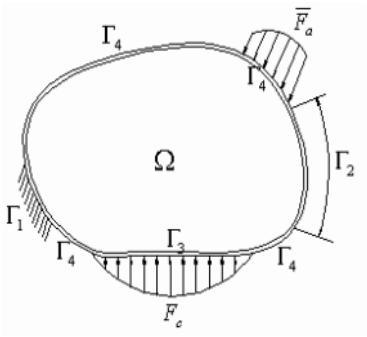

Figure 3.10: Contact model analyze [21].

The stiffness matrix is singular and no unique solution for displacement is possible if the structure is unsupported for the above structure stiffness equation. For this reason all displacement on the boundary $\Gamma_1$are zero, that means U_1=0.When apply this condition to the system matrix and vector in equation 3.11 FEA equation becomes:

Matrix and vector in equation 3.11 FEA equation becomes:

$$\begin{matrix} K_{22} & K_{23} & K_{24} \\ K_{32} & K_{33} & K_{34} \\ K_{42} & K_{43} & K_{44} \end{matrix} \begin{matrix} U_2 \\ U_3 \\ U_4 \end{matrix} = \begin{matrix} F_2 \\ Fc \\ F_a \end{matrix} \quad \text{..... 3.12}$$

To calculate the contact forces F_c at U_2. Multiple 3rd row of the stiffness matrix with displacement matrix, then equation became:

$$K_{42}U_2 + K_{43}U_3 + K_{44}U_4 = Fa \quad \text{…….. 3.13}$$

$$U_4 = K_{44}^{-1}[Fa - K_{42}U_2 - K_{43}U_3] \quad \text{……..3.14}$$

Multiple the 2nd a row with displacement column, the equation became;

$$K_{32}U_2 + K_{33}U_3 + K_{34}U_4 = F_c \quad \text{……... 3.15}$$

$$U_3 = K_{33}^{-1}[Fc - K_{32}U_2 - K_{34}U_4] \quad \text{…… 3.16}$$

When equation 3.13 substitute in the equation 3.14, U3 became;

$U_3 = K_{33}^{-1}[F_c - (K_{33} - K_{34} K_{44}^{-1} K_{43}) U_2 - K_{34}K_{44}^{-1} F_a + K_{34}K_{44}^{-1}K_{43} U_3]$ ………… 3.17

Therefore the displacement at the contact point is:

$U_3 = K_{33}^{-1}[F_c - (K_{33} - K_{34} K_{44}^{-1} K_{43}) U_2 - K_{34}K_{44}^{-1} F_a + K_{34}K_{44}^{-1}K_{43} U_3]$ …… 3.18

Generally, the contact between the wheel and rail are considered to determining the failure effect of rail end and rail joint. Stress -strain relationship of structural analysis

$\{ \boldsymbol{\sigma} \} = \{K\} \{ \in^{el}\}$ ………………………………………………………… 3.19

$\in^{el}$, σ and D are elastic strain vector, stress vector and elastic stiffness matrix.

$\{ \boldsymbol{\sigma} \} = \{ \boldsymbol{\sigma}x, \boldsymbol{\sigma}y, \boldsymbol{\sigma}z, \boldsymbol{\sigma}xy, \boldsymbol{\sigma}yz$ and $\boldsymbol{\sigma}xz\}$ ………………………………… …. 3.20

$\{ \in^{el}\} = \{\in\} - \{\in\}^{th}$ ……………………………………………………….3.21

$\{\in\} = \{\in\}^{th} + \{D^{-1}\}\{ \boldsymbol{\sigma} \}$ ………………………………………………… ... 3.22

$$\{D^{-1}\} = \begin{bmatrix} 1/E_x & -v_{xy}/E_x & -v_{xy}/E_x & 0 & 0 & 0 \\ -v_{yx}/E_y & 1/E_y & -v_{yz}/E_y & 0 & 0 & 0 \\ -v_{zx}/E_z & -v_{zy}/E_z & 1/E_z & 0 & 0 & 0 \\ 0 & 0 & 1/G_{xy} & 0 & 0 & 0 \\ 0 & 0 & 0 & 1/G_{yz} & 0 & 0 \\ 0 & 0 & 0 & 0 & 0 & 1/G_{xz} \end{bmatrix} \quad 3.23$$

E_x and G_{xy} are young's modulus in the x direction and shear modulus in the xy plane

V_{xy} and v_{yx} are major poison's ratio and minor poison's

Also the $\{D^{-1}\}$ matrix is presumed to be symmetric, so that

$$\frac{v_{xy}}{E_y} = \frac{v_{xy}}{E_x} \quad \text{………………………………………………………… 3.24}$$

$$\frac{v_{zx}}{E_z} = \frac{v_{xz}}{E_x} \quad \text{…………………………………………………………..3.25}$$

$$\frac{v_{zy}}{E_z} = \frac{v_{yz}}{E_x} \quad \text{……………………………………………………… 3.26}$$

$$\frac{v_{zx}}{E_z} = \frac{v_{xz}}{E_x} \quad \text{……..3.27}$$

$$\frac{v_{zy}}{E_z} = \frac{v_{yz}}{E_y} \quad \text{…….. 3.28}$$

The element integration point strain and stress are:

$\{\in^{el}\}=\{B\}\{U\} - \{\in\}^{th}$, for this case, $\{\in\}^{th}$ is zero …… 3.29

$\{\ \boldsymbol{\sigma}\ \} = \{D\}\{\in^{el}\}$ …….. 3.30

B and$\{\in\}^{th}$ are strain - displacement matrix evaluated at integration point and thermal strain

$\in^{el}$ is strain that cause stress

Maximum stress failure criteria

$$\boldsymbol{\varepsilon_x} = \text{maximum of} \begin{cases} \frac{\sigma_{yc}}{\sigma_{yc}^f}, \frac{\sigma_{xy}}{\sigma_{xy}^f} \\ \frac{\sigma_{yc}}{\sigma_{yc}^f}, \frac{\sigma_{yz}}{\sigma_{yz}^f} \\ \frac{\sigma_{zc}}{\sigma_{zc}^f}, \frac{\sigma_{zx}}{f_{\sigma_{zx}}} \end{cases} \quad \text{…….. 3.31}$$

σ_x, σ_y and σ_z are stress in x, y, z direction

σ_{xc}^f , σ_{yc}^f and z are normal stress failure in x, y, z direction.

σ_{xy}, σ_{xy} andσ_{xy} are shear failure in xy, yz, xz direction.

3.6 Geometrical Model

In the three-dimensional model of rail joint and wheel, single surface of its symmetry in axial direction is not insulated owing nature of considered phenomenon of loading. It has six holes to fasten bolts. The geometry of the rail on CATIA is illustrated in Fig 3.11.

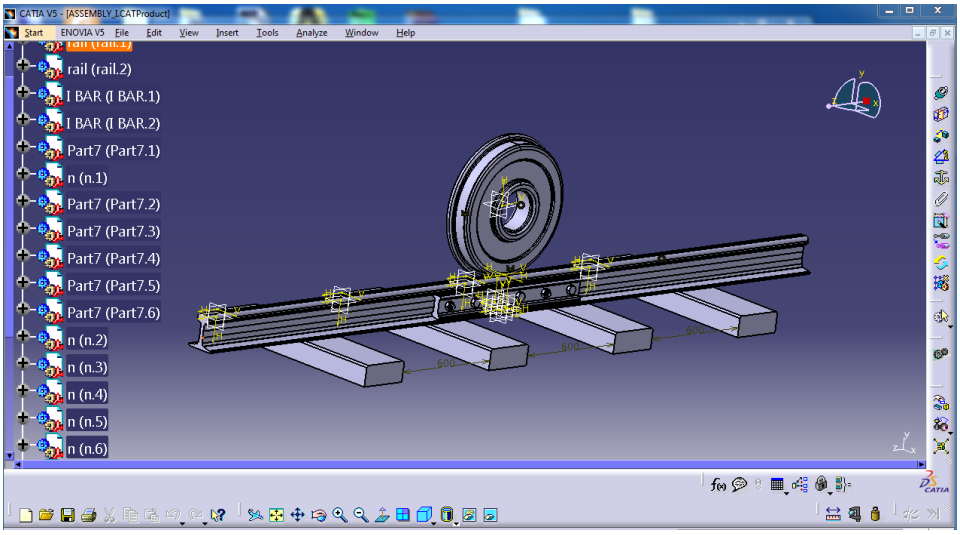

Figure 3.11: 3D model of rail joint

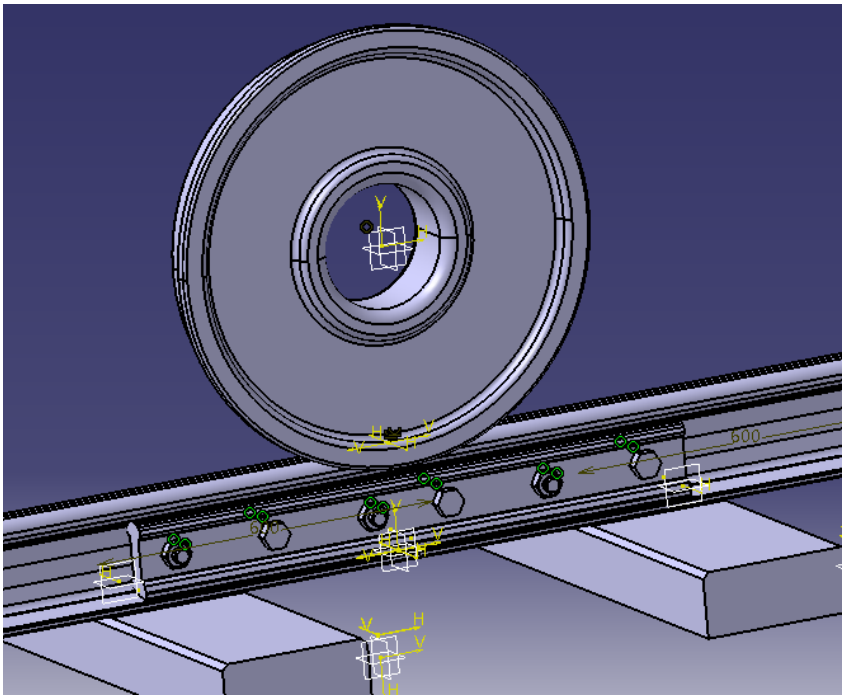

Figure 3.12: 3D model of wheel /rail contact at a rail joint

3.7 Definition of Material

Materials of the rail joint given the principal requirements involved, the steels generally used for wheels and rails have a predominantly pearlitic microstructure incorporating hard cementite lamellae that guarantees high resistance to wear. The microstructure produced by transformation close to thermodynamic equilibrium simultaneously ensures more sluggish transformation in operation than, for instance, a bainitic or martensitic microstructure [22]

3.7.1 Materials used

The railway tracks are mostly steel material in accordance to the EN 13674-1:2011 (E). It can be produced with tensile strengths exceeding 5 GPa. Steel contains 50% iron and one or more alloying element.

These elements generally include carbon, manganese, silicon, chromium, phosphorus, sulpher etc. Each element has a specific role in the steel making process or in achieving particular properties E.g. Strength, hardness and quality. Most of the materials used in this specific project are based on Addis Ababa Light rail Transit (LRT). In this study the wheel has approximately similar material properties to the rail. Properties of joint bars and rail are the same for the simplicity of the problem, but for the concrete sleepers with a density of 2300kg/m3.

Table 3.5: Mechanical property of rail material

Item No	Mechanical property	value
1	Poison'sRatio	0.3
2	Young's Modulus (MPa)	207 MPa
3	Ultimate tensile strength (MPa)	880 MPa
4	Yield strength	640 MPa
5	Density	7800 kg/m
6	Elongation	12 %

Table 3.6: Mechanical property of *Concrete* material

	Young's modulus, MPa	*Poisson's ratio*	*Density, kg/m3*
Concrete	*300000*	*0.18*	*2300*

Table 3.7: Chemical composition of rail

Item No	1	2	3	4	5	6
Chemical element	C	Si	Cr	Mn	p	s
composition	0.8	08	---	1	0.04	0.05

Table3.8: Mechanical property of joint washer, bolt and nut

Item No	Mechanical property	value
1	Poison'sRatio	0.3
2	Young's Modulus (MPa)	207 MPa
3	Ultimate tensile strength (MPa)	880 MPa
4	Yield strength	640 MPa
5	Density	7800 kg/m
6	Elongation	12

3.8 Load and Support

Material properties and data are used based on Ethiopia Railway Corporation, Addis Ababa Light rail Transit (LRT). Vertically downward load is sum of 3% allowance, maximum axle load. The overall load is the sum of the total tram weight and carrying capacity of the vehicle. The overall load is classified to each axle of the vehicle then the axle load is classified to each

wheel vehicle. Carrying capacity of vehicle has calculated by take average of 60kg/ person and the total rate of passenger inside of the tramcar is 317.

Table 3.9: Seating capacity of vehicle

Item No	Number of passengers (persons)	Seated	Standing	Total
1	Seats (AW_1)	60	5	65
2	Seating capacity (AW_2) (standing: 6 persons/m^2)	65	190	254
3	Overload capacity (AW_3)(standing: 8 persons/m^2)	65	252	317

Table 3.10: Vehicle weight

Item No	Loads	Carbody weight	Passenger weight	Total weight
1	Empty vehicle (t)	44	0	44
2	Seating capacity (t)	44	15.24	59.24
3	Overload capacity (t)	44	19.02	63.02
4	Axle load	≤11（1+3%）t		
5	Axle number	6		

Note: Take 60kg as average weight of each passenger.

3.9 Analysis of Straight Rail Joint Using ANSYS 14.5

3.9.1 Meshing

In the finite element analysis the basic concept is to analyze the structure, which is an assemblage of discrete pieces called elements, which are connected, together at a finite number of points called nodes. A network of these elements is known as a mesh. For this analysis, the model of rail joint was meshed with the tetrahedral finite element were used in ANSYS rather than defining the nodes individually (fig.3.13). The finite elements used for the meshing were Free triangular. The size of the meshing type is medium size mesh.

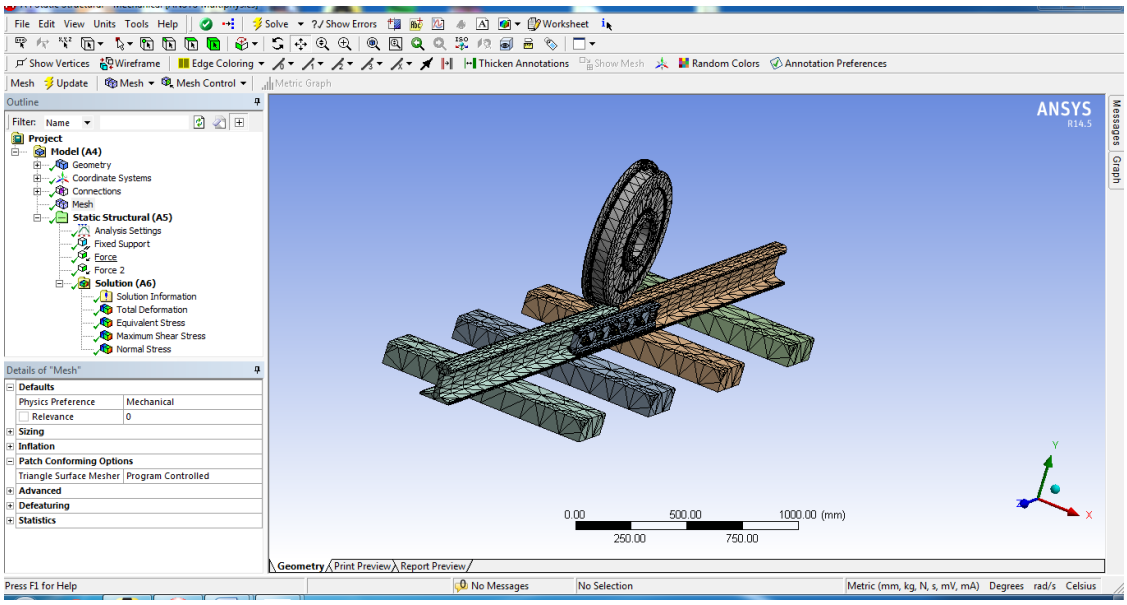

Figure 3.13: Meshed Model of rail joint

3.9.2 Finite element simulation computation model

A 3-D finite element model for element model for wheel/rail rolling contact is developed on the most critical section of rail track i.e., rail joint to calculate finite element analysis and stress response in the contact region.

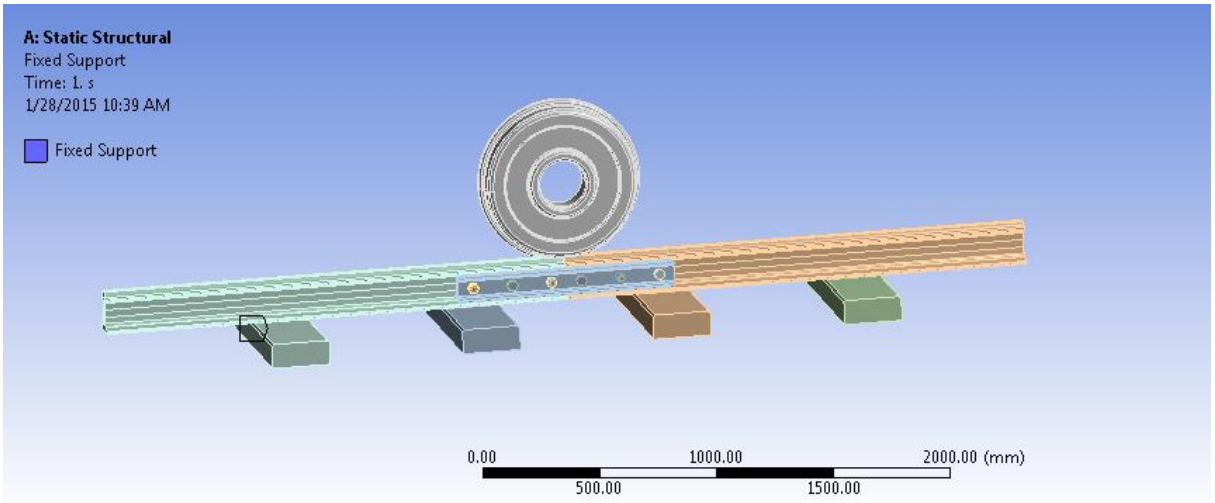

Figure3.14: Finite element modeling of wheel rail set

3.9.3 Wheel load

In this model, the load is the static load on wheel, which is applied on the center of wheel. The position of applied load and direction on wheel are shown in Figure 3.15. But in case of the tram car we do have three bogies each having two axles and the wheel load will be one half of the weight of the axle load. The total numbers of the axles are six.

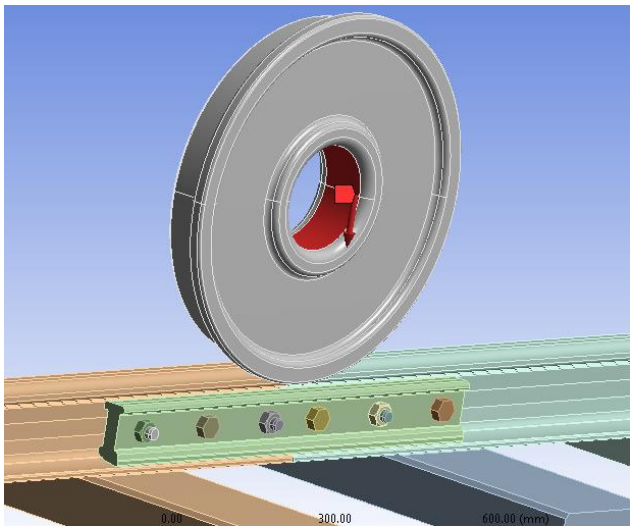

Figure 3.15: the position of applied wheel load

The total vertical load is calculated as follows:

a. Tram car weight = 44 ton
   - The load apply on each axle = 7.333 ton = 73333N
   - The load apply on each wheel = 3.667 ton = 36667 N

b. Carrying Capacity = 60kg/person *317 person = 19020N
c. Over all capacity = Tram car weight on each wheel + Carrying Capacity
d. Maximum Axle load = 11,000 kg $\times$ $9.81 m/s$
   =107,910N
e. The total vertical load = maximum Axle load +3% maximum Axle load
   = 111147.3N
f. The load on each wheel = 55573.63N

3.9.4 Velocity on wheel

As the wheel is rolling on the top of rail, its velocity has two components, namely the moving velocity and angular velocity. Their relationship is that, the product of angular velocity magnitude and radius of the wheel equals to the magnitude of moving velocity.

Table 3.11: Operating speed of tram

Item No	Parameter	Speed
1	Maximum operation speed	70 km/h
2	Average travelling speed	≥20km/h
3	Operation speed during car wash	3~4 km/h

The maximum operation speed of the tramcar is 70km/h and Wheel diameter is 660mm then the rotational velocity can be calculated as:

From V=wr, $w = \frac{v}{r}$ =70km/h /330mm =58.9225rad/s

3.9.5 Boundary conditions

To ensure to achieve the satisfactory results, some constraints should be applied to the components. The surfaces which need to be constrained are shown as solid filled areas in Figure 3.16. All the material properties and boundary conditions are being applied strictly as per the guidelines made available according to the researcher. The wheel runs at constant speed of 70 km/hr. UIC 50 rail is used for analysis. The initial temperature of wheel and rail is taken as $22C^{0,}$ for analysis in ANSYS Friction coefficient is 0.15[41]. The material's density is 7800 kg/m3. Material properties of the rail and wheel are assumed to be same. The diameter of wheel is 660 mm. The axle load is 111147.3N Figure below shows boundary conditions and load conditions on rail joint.

The types of loading that can be applied in a static analysis include:

- Vertical wheel load (force).
- Standard earth gravity
- Rotational velocity

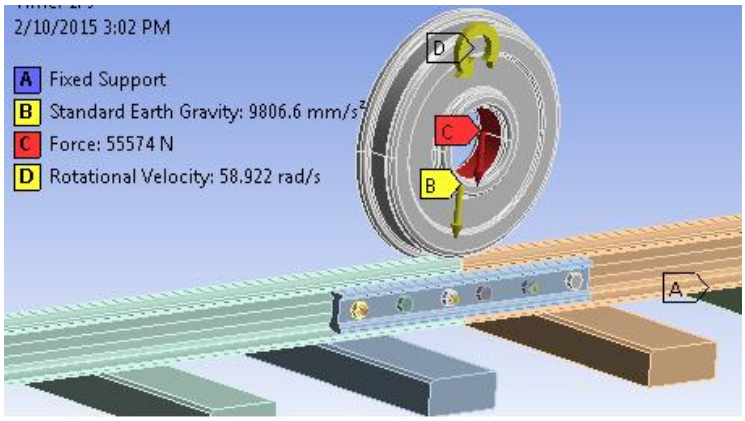

Figure 3.16: the boundary conditions of supports on FE model

Note: The maximum axle load is taken to perform the analysis

CHAPTER FOUR

RESULT AND DISCUSSION

4.1 Results

The analysis is performed by using finite element model consist of fatigue analysis, to determine the impact of the wheel load on a bolted rail joint. Different support location is used to perform finite element analyses, although the geometry and load application are the same for all support location.

4.1.1 Static Analysis

A static structural analysis is determine the deflection, stresses, strains, safety factor, and fatigue stress of structures caused by loads that do not induces significant inertia and damping effects. The load and the structure responses are assumed to vary slowly with respect to time that means steady loading and response condition are assumed.

4.1.1.1. Stress

Stress is defined as the average force per unit area that some particle of a body exerts on an adjacent particle, across an imaginary surface that separates them.

I) Equivalent (von- miss) stress (MPa)

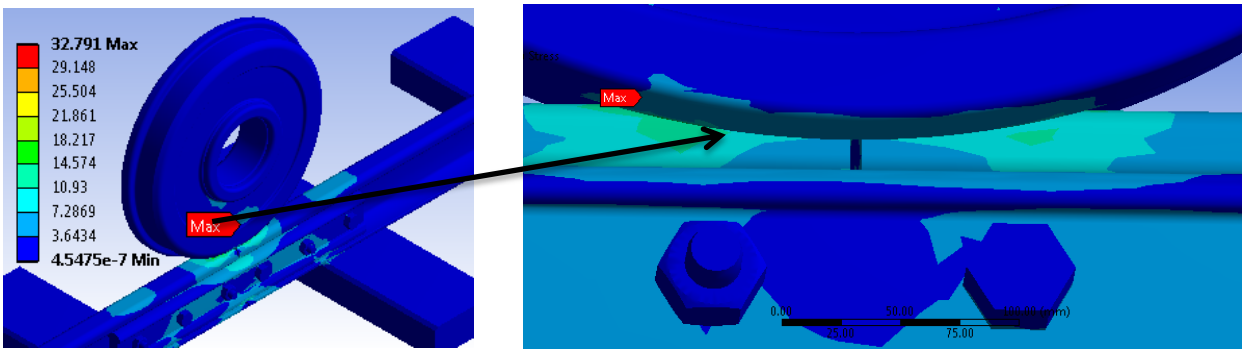

Figure 4.1: Von miss stress.

As shown in above figure, the maximum von miss stress is 32.791MPa and the minimum von miss stress is $4.5475e^{-5}$MPa,

II) shear stress in MPa

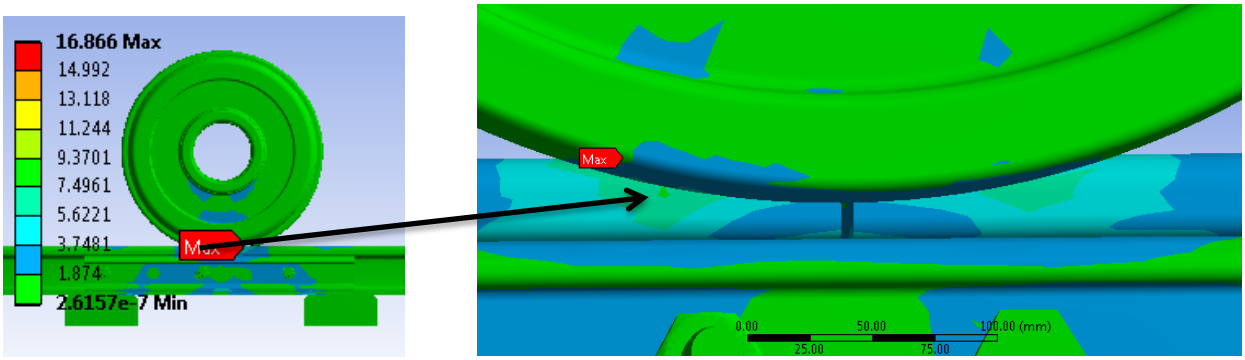

Figure 4.2: shear stress

As shown in the above the max shear stress is 16.866MPa and the min shear stresss is $2.6157e^{-5}$

III) Normal stress

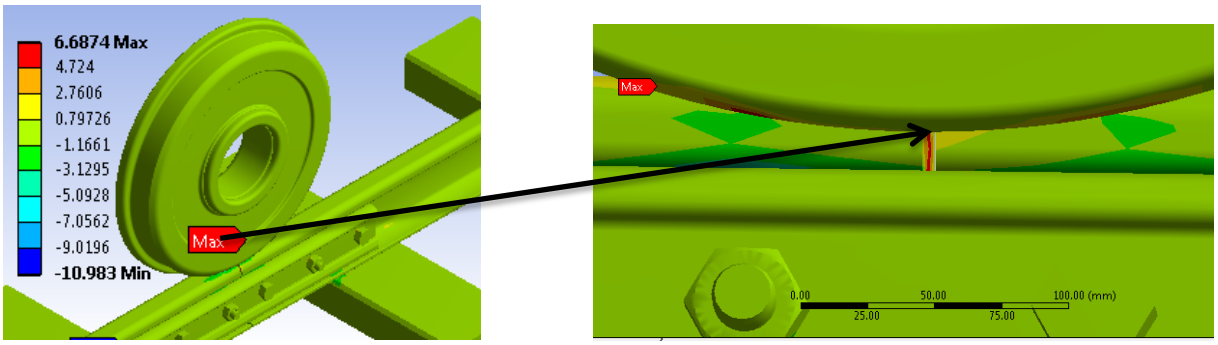

Figure 4.3: Normal stress (bending stress)(Mpa)

As shown in above figure, the maximum normal stress is6.6874MPa and the minimum normal is -10.983MPa,

The table below shows the comparing the different stress values of research result values of JBG1 and JBG2 using same tram car wheel load.

Table 4.1: von miss stress shear stress and normal stress values of the JBG1 and JBG2 at the rail ends of each side.

Von mises stress(MPa)	Max Min	105.86 0.0087346	32.791 $4.5475e^{-7}$
Shear stress(MPa)	Max Min	10.661 -10.751	16.866 $2.6157e^{-7}$
Normal stress(MPa)	Max Min	22.26 -38.536	6.6874 -10.983

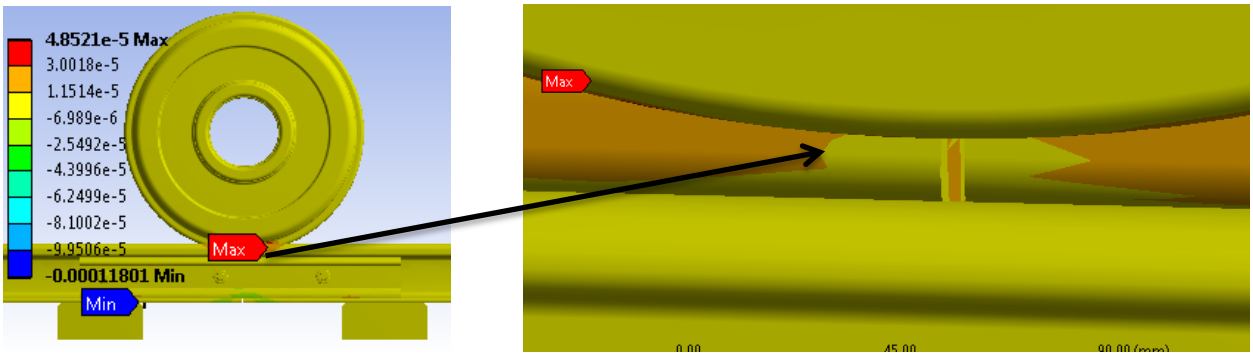

Figure 4.4: Equivalent elastic strain

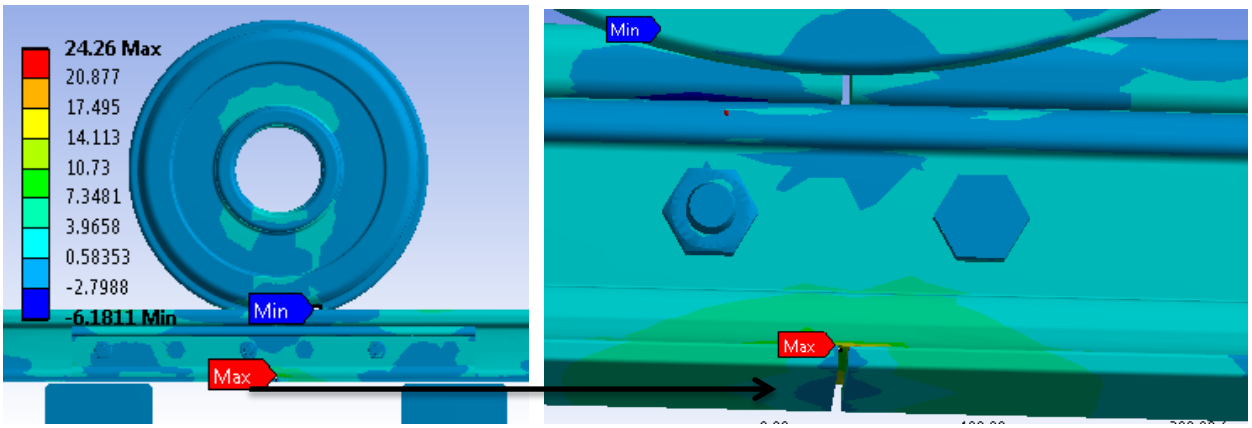

Figure4.5:Maximum principal stress

4.1.1.2. Fatigue stress

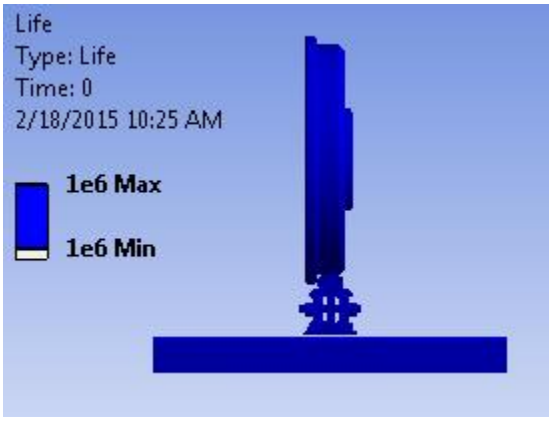

Figure4.6:Fatigue life(In cycles)

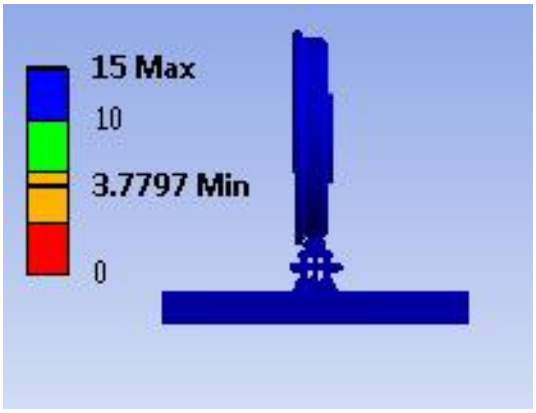

Figure4.7: safety factor

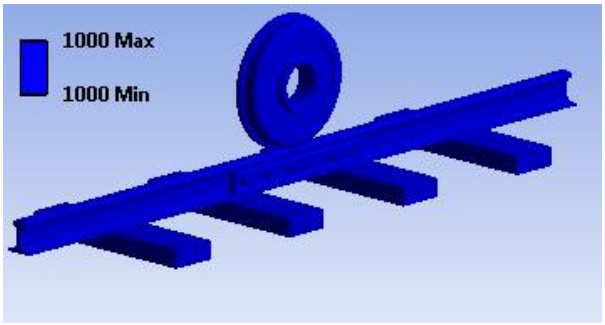

4.8: Fatigue damage

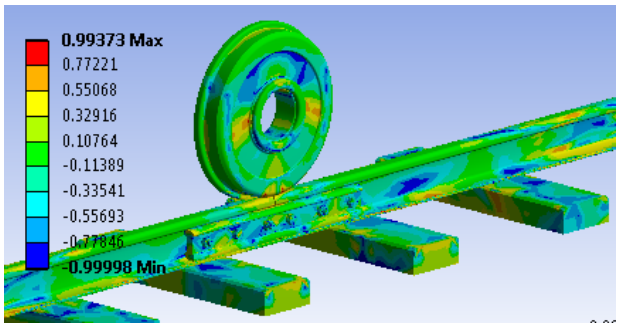

Figure4.9: Biaxiality indication

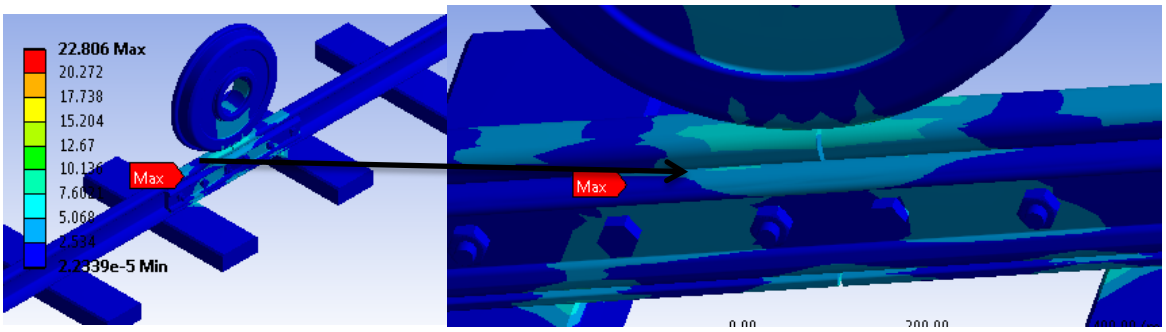

Figure 4.10: Equivalent alternating stress

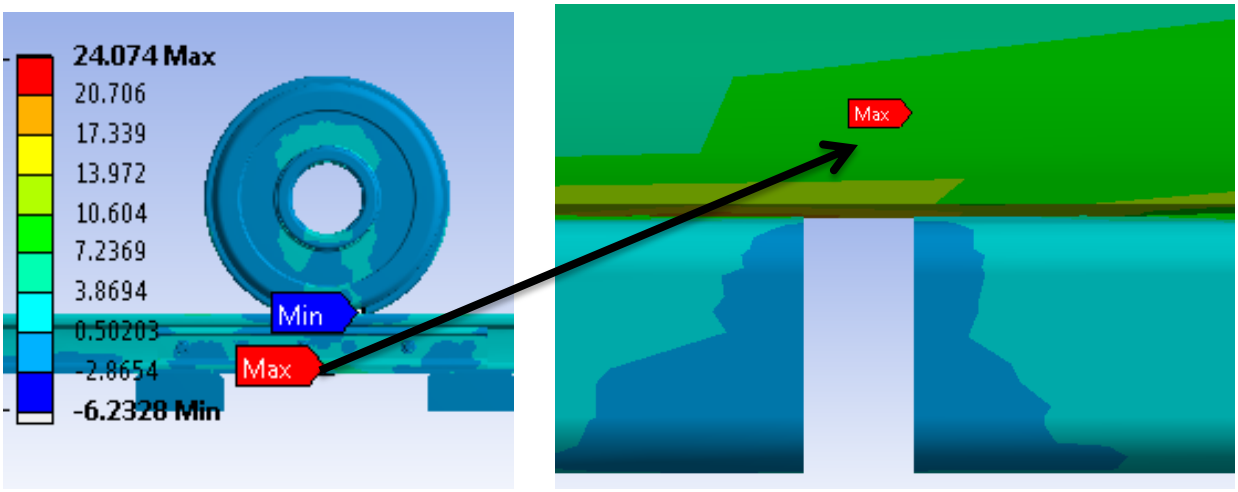

Figure 4.11: Maximum principal values

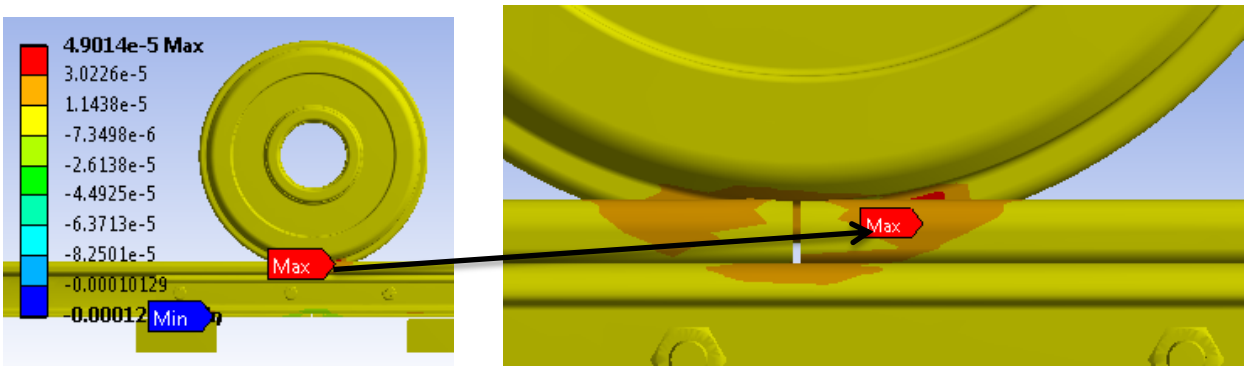

Figure 4.12: Normal elastic strain

4.2 Discussion

A three-dimensional finite element model is used to analysis the rail joint section of track. The finite element program ansys is used to model the joint analysis. This ANSYS is used to simulate the loading and boundary conditions of the rail and wheel contact for a stress analysis. This section of the paper specifies the result obtained from the ANSYS software based on hertz contact theory. The von miss stresses, maximum shear stress and Equivalent elastic strain have been determined under the influence of axle load.

Table4.2: Static stress result summary [32]

Analysis type	Type of load		Case1	Case2	Case3
Static analysis	Von mises stress(Pa)	Max.	$1.88e^7$	$1.029e^7$	$10.58e^7$
		Min.	87.22	332.69	8739.6
	Normal stress(Pa)	Max.	$6.28e^6$	$4.34e^6$	$2.22e^7$
		Min.	$-9.544e^6$	$-4.60e^7$	$-3.853e^7$
	Shear stress(Pa)	Max.	$3.869e^6$	$2.76e^6$	$1.066e^7$
		Min.	$-2.14e^6$	$-3.33e^6$	$-1.075e^7$
	pressure(Pa)	Max.	$2.432e^8$	$2.904e^8$	$1.99e^9$
		Min.	$-7.1e^8$	$-2.59e^9$	$-6.5976e^9$
	Alternating stress (Pa)	Max.	$1.88e^7$	$1.029e^7$	$2.226e^7$
		Min.	87.22	332.69	$-3.85\ e^7$
	Biaxial induction	Max.	0.987	0.994	0.988
		Min.	-0.999	-0.998	-0.999
	Safety factor	Max.	15	15	15
		Min.	0.1429	2	0.81428

Table 4.3: stress results for the research JBG1 AND JBG2

Analysis type	Type of load		Case3 of the JBG1	JBG2
Static analysis andfatigue	Von mises stress(Pa)	Max.	$10.58e^7$	$32.791e^6$
		Min.	8739.6	$1.008e^4$
	Normal stress(Pa)	Max.	$2.22e^7$	$4.1676e^6$
		Min.	$-3.853e^7$	$-7.1595e^6$
	Shear stress(Pa)	Max.	$1.066e^7$	$12.51e^6$
		Min.	$-1.075e^7$	$3.0526e^6$

	Safety factor	Max.	15	15
		Min.	0.81428	3.77185
	Alternating stress (Pa)	Max.	$2.226e^{7}$	$20.316e^{6}$
		Min.	$-3.85\ e^{7}$	$1.00084e^{6}$

CHAPTER FIVE

CONCLUSION RECOMMENDATION AND FUTURE WORK

5.1 Conclusion

Relatively simple models of rail wheel were used for static analysis of the research. The prescribed method in this research may be used to estimate the fatigue life of bolted rail joints in a variety of conditions. The finite element model for reverse bending calculates joint bar bending stresses that are comparable to the engineering estimates based on beam on elastic foundation

In this study, the responses of a bolted rail joint component are determined under static, the results are assumed to be significant. The analysis can include stress, strain and fatigue responses of bolted rail joint caused by vertical wheel load. The load applied is only when the rail joint is in between the sleepers. The stress value is reduced for the new geometry.

5.2 Recommendation

During the joint analysis Joint between the rails needed more attention than other parts, to reduce the problem related to the rail joint. This paper recommends that during the analysis of rail joint the position of the study is when the joint is between the sleepers. For the similar problem engineers can develop the solutions by modification of the geometry of rail joint component part Since rail joint is the weakest spots in the railway track and Rail joint are used to connect the ends of two rails horizontally and vertically it needs special attention. The continuity of the railway track is breaks due to the existence of rail gap and difference in the height of the rail heads. Because of the above reasons rail joints are weaker than the rails and subjected to large stress.

5.3 Future Work

In this paper the stress caused by vertical wheel load and some results of rail joints are obtained for only when the rail joint is between the sleepers. This paper studies mainly on finite element analysis, but to improve the problem related to the joint, it is also needed field data to identify the results for the problems.

The Joint part of the rail track needs more attention to eliminate problem related to the wheel/ rail contact like fracture of rail and joint bar hole, looseness of bolt, nut, and dislocation and distorted of the rail joints.

To minimize the rail and joint wear, the looseness of bolt and nut, and safety problem issues and maintenance cost of the railway track. It is also good to study and see more on following area:

- Study the Cause of stress on rail joint due to thermal, lateral force and longitudinal force.
- Study on the effect of vibration on the joint part of the rail
- Developing materials with cyclic load resistance.
- Analysis stress of bolt and nut at joint by adding toque.
- Developed strong material for bolt and nut and rail hole.
- Testing and investigating of materials of components of the rail joint
- Identifying the crack initiation at rail hole.
- Identifying the stress by changing the bolt geometry.

APPENDIX

1. Strain amplitude (in log scale)

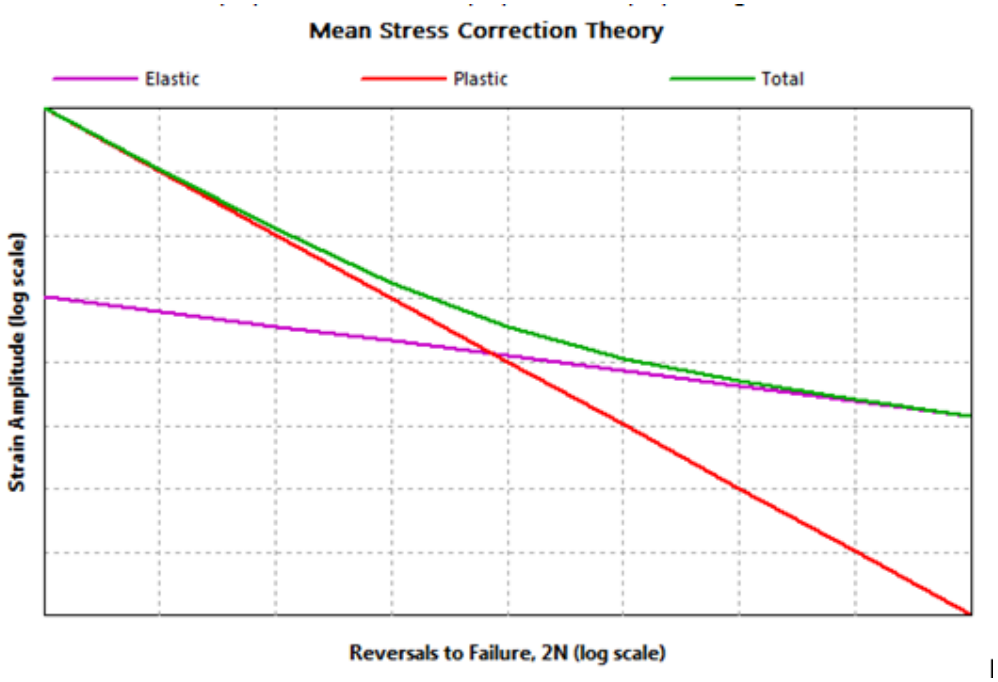

Figure 5.1 Strain amplitude (in log scale)

4 Constant amplitude load

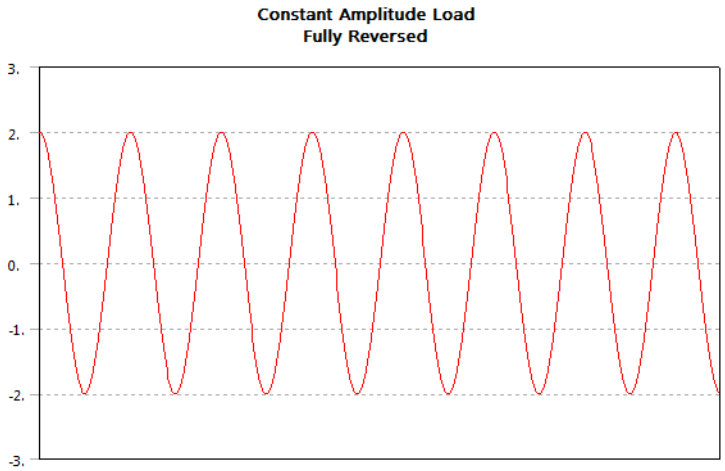

Figure 5.2: Constant load amplitude

3. Mean stress correction

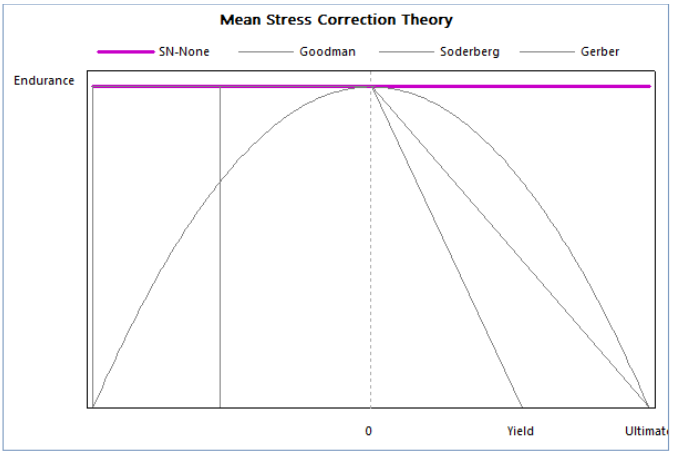

Figure 5.3: Mean stress correction theory

3 Velocity converge

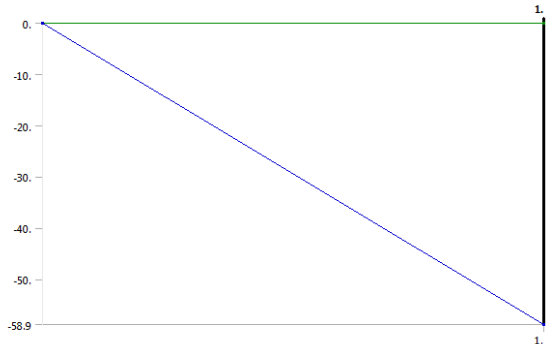

Figure 5.4: Velocity converge

4 Load converge

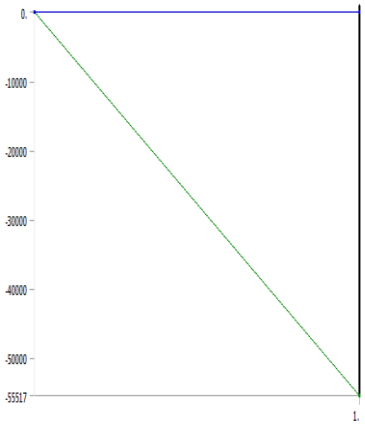

Figure 5.5 : Load converge

References

[1].Igwemezie, J. and Nguyen, A. "Anatomy of joint bar failures ." Railway Track and Structures July 2009: 31-37

[2]. Himebaugh, A. K. "Finite Element Analysis of Insulated Railroad Joints." MS thesis. Virginia Polytechnic Institute and State University. 28 November 2006.

[3].Hetényi, M. "Beams on Elastic Foundation: Theory with applications in the fields of civil and mechanical engineering." Ann Arbor: The University of Michigan Press. 11th Printing, 1979.

[4].Igwemezie, J. and Nguyen, A. "Anatomy of joint bar failures I." Railway Track and Structures July 2009: 31-37

[5] Hiroo KATAOKA, Noritsugi ABE and Osamu Wakatsuk, *Evaluation of Service Life of Jointed Rails*, Track Structure & Component Group, Railway Technical Research Institute, Japan

[6] Anne K. Himebaugh, November 28, 2006,*Finite Element Analysis of Insulated Railroad Joints,* Master of Science In Civil Engineering,1-75

[7] Daniel Peltier, Christopher P. L. Barkan, Engineering Steven Downing and Darrell Socie, *Measuring Degradation of Bonded Insulated Rail Joints* , University of Illinois at Urbana-Champaign Urbana, IL 61801

[8]Jenkins, H. H.; Stephenson, J. E.; Clayton, G. A.; Morland, G. W.; and Lyon, D.
"The effect of track and vehicle parameters on wheel / rail vertical dynamic forces", Railway Engineering Journal, v3, n1, Jan, 1974, p 2-16.

[9] Kerr, Arnold D. and Cox, Joel E. "Analysis andtests of bonded insulated rail joints subjected to vertical wheel loads," *International Journal of Mechanical*
Sciences, v 41, n10, Oct, 1999, p 1253- 1272.

[10]. Akhtar, M., Davis, D.D and O'Connor, T. (2008) Revenue service evaluation of advanced design insulatedjoints, *Proceedings of the AREMA 2008 Annual Conference*, September 21-24, Salt Lake City, Utah,USA

[11] Akhtar, M.N. and Davis, D.D. (2008) Preliminary results of prototype insulated joint tests at the Facility for Accelerated Service Testing, U.S. Department of Transportation, Federal Railroad Administration, RR08-11.

[12]. Peltier, D., Barkan, C.P.L., Downing, S., Socie D. (2007) Measuring degradation of bonded insulated rail joints, *Proceedings of the AREMA 2007 Annual Conference*, Chicago, IL,

USA.

[13]. Peltier, D., Barkan, C.P.L., Downing, S., Socie D. (2007) Using strain gauges to detect epoxy debonding in insulated rail joints, Proceeding of International Heavy Haul Conference Specialist Technical Session – High Tech in Heavy Haul , Kiruna, Sweden, June 2007, 151-158.

[14]. Peltier, D. and Barkan, C.P.L. (2008) Modeling the effects of epoxy debonding on bonded insulated rail joints subjected to longitudinal loads, Proceedings of the TRB 87th Annual Meeting, Washington, DC (January 2008).

[15] [International Journal of Research in Engineering and Technology _Jan-2013]

[16]Jeong, D.Y., "Progress in Rail Integrity Research," Volpe Center Final Report to Federal Railroad Administration, DOT/FRA/ORD-01/18, October 2001.

[17] Pang, T. (2007) Studies on wheel/rail contact - impact forces at insulated rail joints, Master of Engineering Thesis, Centre for Railway Engineering, Central Queensland University, Australia

[18] Chen, YC & Kuang, JH 2002, 'Contact Stress Variations Near the Insulated Rail Joints', Proceedings of the Institute of Mechanical Engineers, Part F, Journal of Rail and Rapid Transit, 216, pp. 265-274.

[18a] Zong, N, Askarinejad, H, Bandula-Heva, T & Dhanasekar, M 2013, 'Service Condition of Railroad Corridors around the Insulated Rail Joints', *Journal of Transportation Engineering, ASCE*, 139(6), pp. 643-650.

[19] Addisu Negash, October, 2012, *Analysis of Wheel/Rail Contact Geometry and Applied Load Conditions on the Rail Head Surface*, Addis Ababa university, Addis Ababa Ethiopian

[20] IWNICKI, 2003. Simulation of wheel–rail contact forces. s.l.:Fatigue & Fracture of Engineering Materials & Structures.

[21] Jiangtao Song and Randy J Gu, 01 - 05 June 2008 *A Finite Element Based Methodology for Inverse Problem of Determining Contact Forces Using Measured Displacements*,International Conference on Engineering Optimization.

[22] W. Yan and F. D. Fischer ,*Applicability of the Hertz contact theory to rail-wheel contact problems,* Archive of Applied Mechanics 70 (2000) 255±268

[23] E. Kabo, J. C. O. Nielsen, and A. Ekberg. Prediction of dynamic train-track interaction and subsequent material deterioration in the presence of insulated rail joints. Vehicle System , 44:718–729, 2006.

[24] Y.-C. Chen and L.-W. Chen. Effects of insulated rail joint on the wheel/rail contact stresses under the condition of partial slip. Wear, 260:1267–1273, September 2006.

[25]Y.-C. Chen and J. H. Kuang. Contact stress variations near the insulated rail joints. Proc Inst Mech Eng Part F J Rail Rapid Transit, 216:265–274, 2002.

[26] FRA's accident data, a total of accidents related to joint failures occurred from 2000 to 2009

[27]Akhtar, M.N. and Davis, D.D. (2008) Preliminary results of prototype insulated joint tests at the Facility for Accelerated Service Testing, U.S. Department of Transportation, Federal Railroad Administration, RR08-11.

[28]Parsons Brinckerhoff, 2012:"Track Design Handbook for Light Rail Transit" Second Edition, National Academy of Sciences ,4-7-4-108.washington, d.c.

[29]Coenraad Esveld, 2001: Modern Railway Track "2nd edition, MRT production,1-660

[30] Different joint bar geometry types www.jointbartypes

[31] Bruzek, R., Jamieson, D., "Field Activities for Joint Bar Failure Study, Phase 1," ENSCO Final Report to Federal Railroad Administration, ENGR-REPT-0000136, September 2012

[32] Thesis in engineering and technology in railway engineering in stress analysis of bolted rail joint _Jan- 2014

[33] Federal Railroad Administration, Railroad Accident/Incident Reporting System (RAIRS). http://safetydata.fra.dot.gov/officeofsafety/default.aspx

[34] Brandon T., David Y.J. and Jeff G., Estimation of The Fatigue Life of Railroad Joint Bars, 2007 ASME/IEEE, USA, Joint Rail Conference and Internal Combustion Engine Spring Technical Conference (JRCICE – 2007), held at Pueblo, Colorado, USA, during March 13-16, 2007.

[35]Nirmal. Mandal, M. Dhanasekar, P. Boyd, Shakedown stress analysis of insulated rail joint (IRJ), Proceedings of the 8th International Conference on Contact Mechanics and Wear of Rail/Wheel System, Florence, Italy. (2009) 783-793.

[36] Lichtberger, B. *Track compendium.(2007) Eurorailpress VA Profillidis. Railway management and engineering(2009) Asgathe.*

[37]Cox, Joel E. *Rail Joint Mechanics*. Master's Thesis, Department of Civil Engineering, University of Delaware, 1993.

[38] Li, Dingqing, William Shust, and Semih Kalay. February 1997. "Track Panel Shift due to Repeated Passes of Lateral Axle Loads." *Technology Digest* TD-97-006, Association of American Railroads, Transportation Technology Center, Inc., Pueblo, CO.

[39] Second Edition, National Academy of Sciences ,4-7-4-108.washington, d.c. W. Yan and F. D. Fischer ,*Applicability of the Hertz contact theory to rail-wheel contact problems,* Archive of Applied Mechanics 70 (2000) 255±268

[40] Johnson, K. L. (1985) ,*Contact Mechanics*, (Cambridge University Press, Cambridge)

[41] Bos J., *Frictional Heating of Tribological Contacts*. Ph. D. Diss., Univ. of Twente, Enschede, The Netherlands, 1995.